Silane-functionalized polyionenes-coated cotton fabrics with potent antimicrobial and antiviral activities

Qiaohua Qiu [a,b,c,1], Chuan Yang [a,1], Yanming Wang [a], Cherylette Anne Alexander [a], Guangshun Yi [a], Yugen Zhang [a], Xiaohong Qin [b,**], Yi Yan Yang [a,*]

[a] Institute of Bioengineering and Bioimaging, 31 Biopolis way, Singapore, 138669, Singapore
[b] Key Laboratory of Textile Science & Technology of Ministry of Education, College of Textiles, Donghua University, Shanghai, 201620, China
[c] College of Textile Science and Engineering, Zhejiang Sci-Tech University, Hangzhou, 310018, China

ABSTRACT

Bacterial and viral infections are posing a huge burden on healthcare industry. Existing antimicrobial textiles that are used to prevent infection transmission are lack of durability and antiviral activity. Here, we report on silane-functionalized polyionenes-coated cotton textiles with durable potent antimicrobial and antiviral activities. To obtain silane-functionalized polyionenes, silane group-containing monomers were synthesized and used to polymerize with co-monomers. These polyionenes were then conjugated onto the surface of cotton fabrics via covalent bonds. These polymers demonstrated broad-spectrum antimicrobial activity against various types of pathogenic microbes as evidenced by low effective concentration. The fabrics coated with these polymers exhibited potent bactericidal ($>$99.999%) and virucidal (7-log PFU reduction) activities. In addition, the antimicrobial efficacy was still more than 92% even after 50 times of washing. Evaluation of cytocompatibility and skin compatibility of the polymer-coated cotton fabrics in mice revealed that they were compatible with cells and mouse skin, and neither erythema nor edema was found in the area that was in contact with the polymer-coated fabrics. The silane-functionalized polyionenes are potentially promising antimicrobial and antiviral coating materials for textiles and other applications to prevent microbial and viral infections.

1. Introduction

Bacterial and viral infections are becoming an increasingly serious threat to public health, and the ability to fend off these threats on a large scale has become an uphill task [1,2]. Many bacterial and viral infections such as COVID-19 are caused by contact [3–5]. Therefore, it is important to use antimicrobial textiles that can prevent the growth of the microbes or even kill them [6,7].

The antimicrobial activity of textiles can be obtained by coating antimicrobial materials onto fabrics through chemical or physical treatments [8,9]. Various antimicrobial agents, such as metal and oxide nanoparticles [10–13], *N*-halamine [14,15], guanidine [16,17], organic quaternary ammonium compounds [18,19], have recently been developed and applied to textiles. In addition, antibacterial materials such as cationic peptide polymers [20,21] have also been used as antimicrobial and antifouling coatings on other surfaces. Among them, cationic antimicrobial agents have received great attention due to their strong antimicrobial activity and prevention of microbial resistance development. Despite considerable progress in developing antimicrobial fabrics in recent years, the ability of these fabrics to retain their antimicrobial activity for a long duration is still a major challenge in the field. Furthermore, the current COVID-19 pandemic has highlighted the need for antiviral fabrics to counter the spread of the virus, of which there has been an evident lack of research into this area. These gaps thus highlight the urgent need to design and develop textiles with both durable antibacterial and antiviral activities.

Polyionenes represent a family of highly effective cationic antimicrobial materials, wherein the quaternized nitrogens are located in the main polymeric chain or backbone of the polymer rather than in pendant groups [22–24]. Polyionenes have low minimum inhibitory concentrations (MICs) and exhibit rapid killing kinetics against a broad spectrum of microbes [25,26]. Additionally, these polymers have also

---

* Corresponding author.
** Corresponding author.

E-mail addresses: xhqin@dhu.edu.cn (X. Qin), yyyang@ibb.a-star.edu.sg (Y.Y. Yang).

[1] These authors contributed to the study equally.
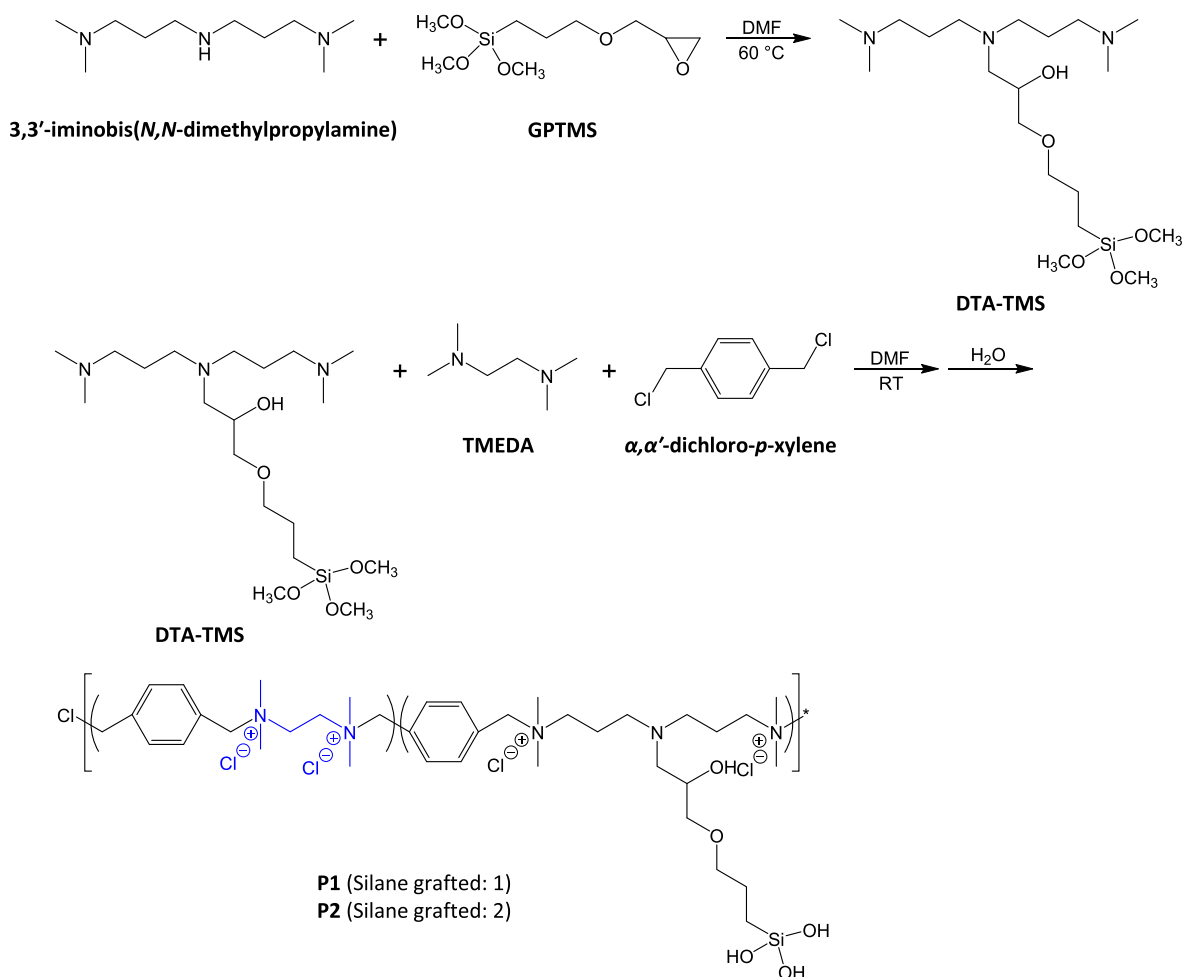
Scheme 1. Synthetic procedures and chemical structures of silane-functionalized polyionene **P1** with one silane group and **P2** with two silane groups.

demonstrated effective mitigation of drug resistance, with superior skin biocompatibility and negligible *in vivo* toxicity [25]. These polymers would thus be a promising candidate for making antimicrobial textiles. While promising in potential, polyionenes are not without weaknesses. A key limitation which needs to be overcome involves the immobilization of polyionenes onto the fabric surface without them leaching out into the environment, for instance, during washing [24]. One of the most effective ways of achieving antimicrobial durability is to design non-dissolution-type antimicrobial polymers, which could be achieved if the antimicrobial polymer chains are covalently attached to surfaces. However, to the best of our knowledge, very few reports were published about the antimicrobial polyionene coating. For instance, Sarah et al. chemically attached polyionenes to a glass surface. This involved several steps, 1) attachment of polydopamine to activate the surface, 2) surface functionalization and 3) *in situ* surface polyaddition reaction to synthesize polyionenes [27]. The initial modification of the substrate may damage the structure of the substrate and change its color, thus limiting its application in textiles. Therefore, it is essential to explore a facile method capable of introducing specific functional groups into the polyionenes, which can form covalent bonds directly with the fabrics under mild conditions. An example of a design incorporating such a method is that of dimethyloctadecyl[3-(trimethoxysilyl)propyl]ammonium chloride (AEM 5700) from Dow Corning Company, in which the antimicrobial agents are covalently bonded onto the surface of the fabric via alkoxysilanes, thereby conferring durable antibacterial activity on the fabric [8,28]. Despite their durable antibacterial activity, antiviral activity of its coating is unknown. In addition, their stability is poor due to the easy self-condensation of relatively rich siloxane groups [28,29]. Its

low molecular weight may lead to skin penetration, resulting in toxic side-effects [30].

Here, we present a robust methodology to create durable antimicrobial and antiviral cotton fabrics by coating silane-functionalized polyionenes that possess excellent microbicidal/virucidal activity and durable stability. The antimicrobial activity and killing kinetics of the polymer-coated cotton fabrics against *E. coli*, *S. aureus*, and *C. albicans* were investigated. Furthermore, the antiviral activity of the coated fabrics was verified with p22 bacteriophages as model virus. In addition, the durability of antimicrobial activity was also examined after different washing cycles. Finally, the *in vitro* cytotoxicity and *in vivo* skin compatibility studies were also conducted to explore the applicability of these antimicrobial and antiviral textiles.

2. Materials and methods

2.1. Materials

All chemical reagents were purchased from Sigma-Aldrich and Tokyo Chemical Industry (TCI), and used as received unless specified otherwise. Microbial broths were prepared using Muller Hinton Broth (MHB) powder (BD Diagnostics). Gram-negative bacteria *E. coli* (ATCC No. 25922), *P. aeruginosa* (ATCC No. 9027), Gram-positive bacteria *S. aureus* (ATCC No. 6538), and fungi *C. albicans* (ATCC No. 10231) were purchased from ATCC (U.S.A.).
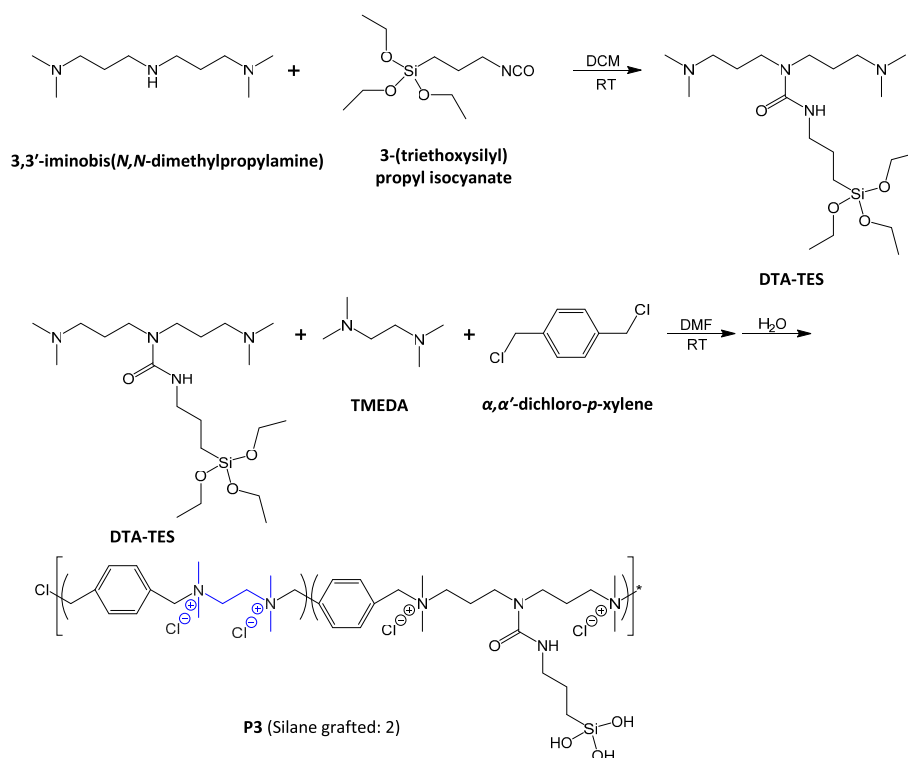
Scheme 2. Synthetic procedures and chemical structure of silane-functionalized polyionene **P3**.

2.2. Polymer synthesis

2.2.1. Synthesis of silane-functionalized polyionenes using (3-glycidyloxypropyl)trimethoxysilane (P1 and P2, Scheme 1)

The experimental procedure for synthesis of cationic polymer **P2** is given below as a typical example. Briefly, (3-glycidyloxypropyl)trimethoxysilane (GPTMS, 0.338 mL, 1.5 mmol) was added dropwise to a 20 mL of vial charged with 3,3-iminobis(*N,N*-dimethylpropylamine) (0.344 mL, 1.5 mmol) in DMF (2 mL) solution under stirring. The reaction solution was heated to 65 °C and reacted overnight. Then, it was cooled down to room temperature and *N,N,N′,N′*-tetramethylethylenediamine (TMEDA, 1.272 mL, 8.5 mmol) was added. α,α′-Dichloro-p-xylene (1.75 g, 10 mmol) in 4 mL of DMF solution was slowly added to the above solution dropwise and then reacted overnight. The reaction solution was precipitated in diethyl ether, centrifuged, and washed with diethyl ether for three times, before drying *in vacuo*, giving rise to a crude product of **P2** as white fine powder. Finally, the polymer was further purified via extensive dialysis against de-ionized (DI) water (molecular weight cutoff (MWCO) of membrane: 1 kDa), and freeze-dried to result in pure **P2** as white solid (Yield, 62%). ^{1}H NMR (400 MHz, D_2O, 22 °C, Fig. S2): δ 7.72 (m, 4 nH, -Ph*H*-), 4.51–4.70 (m, 4 nH, -PhC*H*$_2$-), 4.21 (s, 4 nH, -CH$_2$C*H*$_2$N$^\oplus$(CH$_3$)$_2$-), 3.38 (m, br, 0.49 nH, -C*H*$_2$OC*H*$_2$- of GPTMS), 3.13 (m, 12 nH, –N$^\oplus$(C*H*$_3$)$_2$-), 2.61 (m, br, 0.74 nH, -CH$_2$C*H*$_2$N(C*H*-)C*H*$_2$CH$_2$-), 2.04 (s, br, 0.49 nH, -C*H*$_2$CH$_2$N(CH$_2$-)CH$_2$C*H*$_2$-), 1.59 (s, 0.25 nH, (HO)$_3$SiCH$_2$C*H*$_2$-), 0.56 (s, 0.25 nH, (HO)$_3$SiC*H*$_2$CH$_2$-). Mn$_{GPC}$ = 5120 Da, Đ 1.67.

P1, Yield, 65%; ^{1}H NMR (400 MHz, D_2O, 22 °C, Fig. S1): δ 7.74 (m, 4 nH, -Ph*H*-), 4.54–4.70 (m, 4 nH, -PhC*H*$_2$-), 4.21 (s, 4 nH, -CH$_2$C*H*$_2$N$^\oplus$(CH$_3$)$_2$-), 3.42 (m, br, 0.25 nH, -C*H*$_2$OC*H*$_2$- of GPTMS), 3.16 (m, 12 nH, –N$^\oplus$(C*H*$_3$)$_2$-), 2.62 (m, br, 0.38 nH, -CH$_2$C*H*$_2$N(C*H*-)C*H*$_2$CH$_2$-), 2.13 (s, br, 0.25 nH, -C*H*$_2$CH$_2$N(CH$_2$-)CH$_2$C*H*$_2$-), 1.62 (s, 0.13 nH, (HO)$_3$SiCH$_2$C*H*$_2$-), 0.59 (s, 0.13 nH, (HO)$_3$SiC*H*$_2$CH$_2$-). Mn$_{GPC}$ = 4970 Da, Đ 1.69.
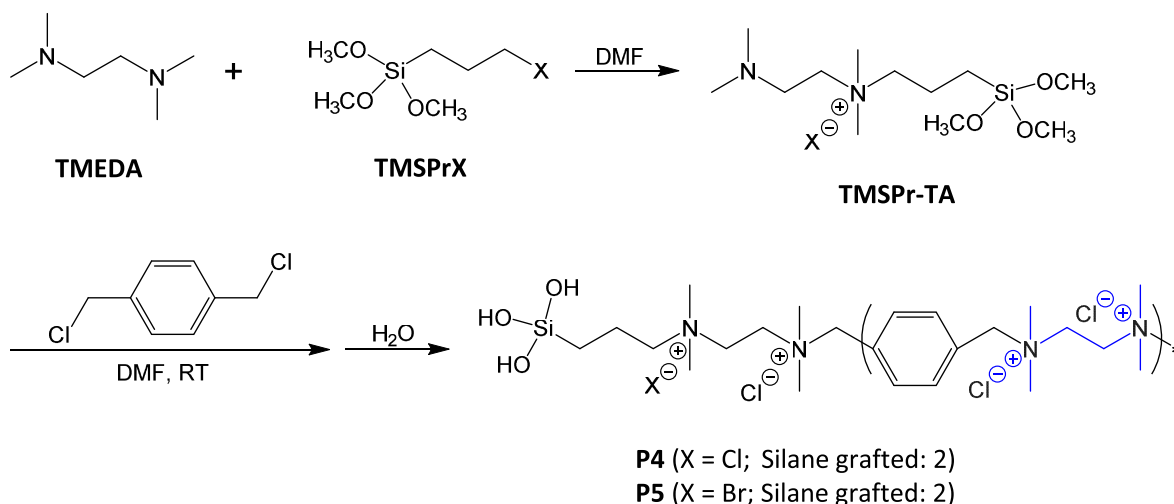
2.2.2. Synthesis of the silane-functionalized polyionene using 3-(triethoxysilyl)propyl isocyanate (P3, Scheme 2)

In a 20 mL of vial, 3,3-iminobis(*N,N*-dimethylpropylamine) (0.688 mL, 3 mmol) and 3-(triethoxysilyl)propyl isocyanate (IPTS, 0.78 mL, 3 mmol) were dissolved in dry DCM (3 mL) and stirred overnight at room temperature under N$_2$ atmosphere. Then, the solution was poured into diethyl ether to precipitate the product, centrifuged and washed with diethyl ether for three times. Finally, the product was dried *in vacuo*, giving DTA-TES as viscous liquid (Yield, 93%). ^{1}H NMR (400 MHz, DMSO-*d*$_6$, 22 °C): δ 6.75 (s, 1H, -CON*H*-), 3.73 (q, 6H, -SiOC*H*$_2$CH$_3$), 3.12 (t, 4H, -CH$_2$C*H*$_2$N(CO)C*H*$_2$CH$_2$-), 2.96 (s, 2H, -CONHC*H*$_2$-), 2.11 (m, 16H, -C*H*$_2$N(C*H*$_3$)$_2$), 1.56 (m, 4H, -C*H*$_2$CH$_2$N(CH$_3$)$_2$), 1.43 (m, 2H, -SiCH$_2$C*H*$_2$-), 1.14 (t, 9H, -SiOCH$_2$C*H*$_3$), 0.51 (s, 2H, -SiC*H*$_2$CH$_2$-).

α,α′-Dichloro-p-xylene (0.875 g, 5 mmol) in 4 mL of DMF solution was added dropwise to a 20 mL of vial charged with the above DTA-TES (0.217 g, 0.5 mmol) and TMEDA (0.674 mL, 4.5 mmol) in DMF (2 mL) solution under stirring and reacted overnight. The reaction solution was then precipitated in diethyl ether, centrifuged, washed with diethyl ether for three times, and dried *in vacuo*, giving crude product of **P3** as a white fine powder. Finally, the polymer was purified using a similar protocol for **P2** purification to obtain the pure **P3** as white solid (Yield, 67%). ^{1}H NMR (400 MHz, D_2O, 22 °C, Fig. S3): δ 7.73 (m, 4 nH, -Ph*H*-), 4.52–4.70 (m, 4 nH, -PhC*H*$_2$-), 4.20 (s, 4 nH, -CH$_2$C*H*$_2$N$^\oplus$(CH$_3$)$_2$-), 3.33 (m, br, 0.65 nH, -C*H*$_2$(-C*H*$_2$)N(CO)NHC*H*$_2$-), 3.14 (m, 12 nH, –N$^\oplus$(C*H*$_3$)$_2$-), 2.11 (s, br, 0.43 nH, -CH$_2$C*H*$_2$N(CO)C*H*$_2$CH$_2$-), 1.49 (s, 0.22 nH, (HO)$_3$SiCH$_2$C*H*$_2$-), 0.53 (s, 0.22 nH, (HO)$_3$SiC*H*$_2$CH$_2$-). Mn$_{GPC}$ = 5570 Da, Đ 1.61.

2.2.3. Synthesis of the silane-functionalized polyionene using (3-halopropyl)trimethoxysilane (P4 and P5, Scheme 3)

The experimental procedure for synthesis of cationic polymer **P4** is given below as a typical example. Briefly, (3-chloropropyl)trimethoxysilane (TMSPrCl, 0.142 mL, 0.75 mmol) and TMEDA (0.749 mL, 5 mmol) were dissolved in DMF (2 mL), in a 20 mL vial and heated to 85 °C

Scheme 3. Synthetic procedures and chemical structures of silane-functionalized polyionene **P4** and **P5**.
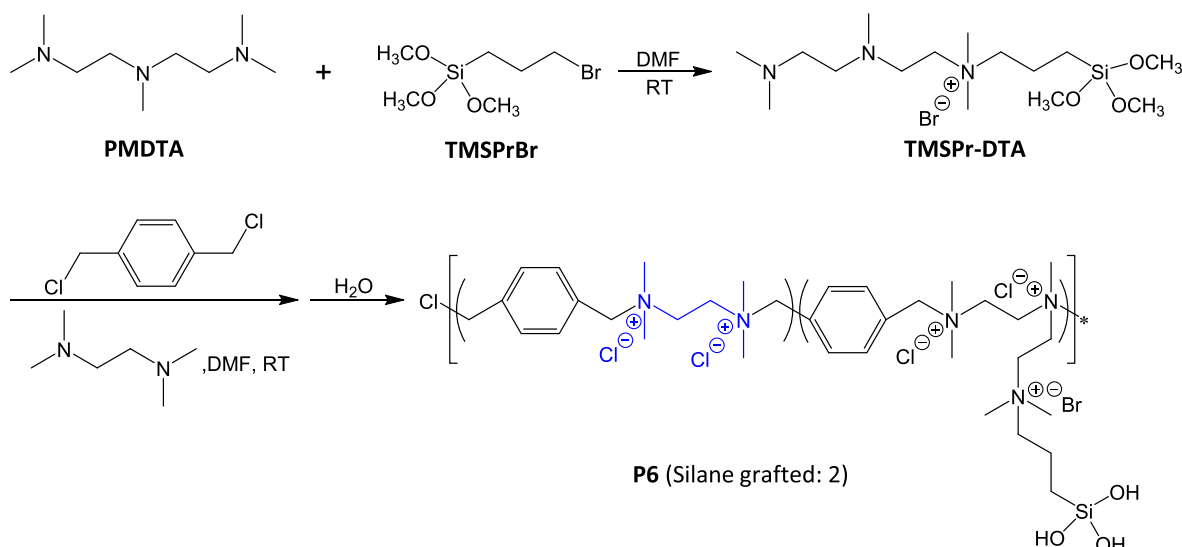
Scheme 4. Synthetic procedures and chemical structure of silane-functionalized polyionene **P6**.

under N_2 atmosphere. The reaction solution was stirred overnight. Then, it was cooled to room temperature and α,α'-dichloro-p-xylene (0.81 g, 4.625 mmol) in 2 mL of DMF solution was slowly added. The reaction continued under stirring overnight at room temperature. The solution was then precipitated in diethyl ether, centrifuged, washed with diethyl ether for three times, and dried *in vacuo*, giving crude product of **P4** as white fine powder. Finally, the polymer was purified using a similar protocol for **P2** purification to yield the pure **P4** as white solid (Yield, 65%). ^{1}H NMR (400 MHz, D_2O, 22 °C, Fig. S4): δ 7.74 (m, 4 nH, -Ph*H*-), 4.70 (s, 4 nH, -PhC*H*₂-), 4.20 (m, 4 nH, -CH₂C*H*₂N⊕(CH₃)₂-), 3.16 (s, 12 nH, –N⊕(C*H*₃)₂-), 1.87 (s, 0.3 nH, (HO)₃SiCH₂C*H*₂-), 0.62 (t, 0.3 nH, (HO)₃SiC*H*₂CH₂-). Mn, $_{GPC}$ = 3330 Da, Đ 1.57.

Similarly, (3-bromopropyl)trimethoxysilane (TMSPrBr) was reacted with TMEDA in excess at room temperature overnight to give TMSPr-TA. **P5** was obtained *via* one-pot reaction as described above. Yield, 61%; ^{1}H NMR (400 MHz, D_2O, 22 °C, Fig. S5): δ 7.74 (m, 4 nH, -Ph*H*-), 4.70 (s, 4 nH, -PhC*H*₂-), 4.18 (m, 4 nH, -CH₂C*H*₂N⊕(CH₃)₂-), 3.16 (s, 12 nH, –N⊕(C*H*₃)₂-), 1.87 (s, 0.33 nH, (HO)₃SiCH₂C*H*₂-), 0.62 (t, 0.33 nH, (HO)₃SiC*H*₂CH₂-). Mn, $_{GPC}$ = 3200 Da, Đ 1.61.

2.2.4. Synthesis of the silane-functionalized polyionene using N,N,N′,N″, N″-pentamethyldiethylenetriamine (PMDTA) (P6, Scheme 4)

PMDTA (1.06 mL, 5 mmol) and 3-trimethoxysilylpropyl bromide (TMSPrBr, 0.38 mL, 2 mmol) were dissolved in dry DMF (3 mL) was dissolved in a 20 mL vial and stirred overnight at room temperature under N_2 atmosphere. The solution was then poured into diethyl ether to precipitate the product, centrifuged and washed with diethyl ether for three times. Finally, the product was dried *in vacuo*, giving TMSPr-DTA (Yield, 85%). ^{1}H NMR (400 MHz, DMSO-d_6, 22 °C): δ 3.50 (m, 4H, -C*H*₂N⊕(CH₃)₂C*H*₂-), 3.34 (s, 9H, -SiOC*H*₃), 3.16 (s, 6H, –CH₂N(C*H*₃)₂C*H*₂-), 2.50 (m, 4H, -C*H*₂N(CH₃)C*H*₂-), 2.35 (m, 2H, -C*H*₂N(CH₃)₂), 2.24 (s, 3H, –CH₂N(C*H*₃)C*H*₂-), 2.15 (s, 6H, –CH₂N (C*H*₃)₂), 1.76 (s, br, 2H, -SiCH₂C*H*₂-), 0.66 (s, 2H, -SiC*H*₂CH₂-).

α,α'-Dichloro-p-xylene (0.595 g, 3.33 mmol) in 4 mL of DMF solution was added dropwise to a 20 mL vial charged with the above TMSPr-DTA (0.208 g, 0.5 mmol) and TMEDA (0.426 mL, 2.83 mmol) in DMF (2 mL) solution under stirring and reacted at room temperature overnight. The reaction solution was precipitated in diethyl ether, centrifuged, washed with diethyl ether for three times, and dried *in vacuo*, giving crude product of **P6** as white fine powder. Finally, the polymer was purified using a similar protocol for **P2** purification to result in the pure **P6** as white solid (Yield, 58%). ^{1}H NMR (400 MHz, D_2O, 22 °C, Fig. S6): δ 7.73

Table 1

Summary of the experimental conditions for antibacterial polymers (nucleophilic addition and quaternization) and antibacterial cotton fabrics.

	Polymer	Silane coupling reagent	Tertiary amine	Fabrics
Nucleophilic Addition	P1	GPTMS	3,3-iminobis(*N,N*-dimethylpropylamine)	F1
	P2	GPTMS	3,3-iminobis(*N,N*-dimethylpropylamine)	F2
	P3	IPTS	3,3-iminobis(*N,N*-dimethylpropylamine)	F3
Quaternization	P4	TMSPrCl	TMEDA	F4
	P5	TMSPrBr	TMEDA	F5
	P6	TMSPrBr	PMDTA	F6

Table 2

Summary of the molecular characteristics for antibacterial polymers.

	Product name	Mn/ PDI[a]	DP of polyionene	Number of silane grafted
Nucleophilic Addition	P1	4970/ 1.69	16	1
	P2	5120/ 1.67	16	2
	P3	5570/ 1.61	18	2
Quaternization	P4	3200/ 2.07	10	2
	P5	3330/ 2.00	11	2
	P6	2890/ 2.02	9	2

[a] Number-Average molecular weight (Mn) and Polydispersity (PDI) values of the polymers were determined by aqueous GPC.

Table 3

MICs of the polymers.

	Product name	*E. coli* (µg/mL)	*S. aureus* (µg/mL)	*P. aeruginosa* (µg/mL)	*C. albicans* (µg/mL)
Nucleophilic Addition	P1	7.81	3.91	7.81	3.91
	P2	7.81	3.91	15.63	3.91
	P3	7.81	7.81	7.81	3.91
Quaternization	P4	7.81	7.81	7.81	3.91
	P5	7.81	3.91	7.81	3.91
	P6	7.81	7.81	7.81	3.91

Table 4

MBCs of the polymers.

	Product name	*E. coli* (µg/mL)	*S. aureus* (µg/mL)	*P. aeruginosa* (µg/mL)	*C. albicans* (µg/mL)
Nucleophilic Addition	P1	7.81	7.81	7.81	7.81
	P2	7.81	7.81	15.63	3.91
	P3	7.81	7.81	15.63	7.81
Quaternization	P4	15.63	7.81	31.25	15.63
	P5	7.81	7.81	7.81	7.81
	P6	7.81	7.81	7.81	7.81

(m, 4 nH, -Ph*H*-), 4.55–4.70 (m, 4 nH, -PhC*H*$_2$-), 4.19 (s, 4 nH, -CH$_2$C*H*$_2$N$^\oplus$(CH$_3$)$_2$-), 3.14 (m, 12 nH, –N$^\oplus$(C*H*$_3$)$_2$-), 1.68 (s, 0.33 nH, (HO)$_3$SiCH$_2$C*H*$_2$-), 0.58 (s, 0.33 nH, (HO)$_3$SiC*H*$_2$CH$_2$-). Mn$_{GPC}$ = 2890 Da, Đ 2.02.

2.3. Preparation of silane-functionalized polyionene-coated cotton fabrics

Cotton fabrics were ultrasonically washed for 1 h using acetone and alcohol, and then rinsed several times using DI water. The fabrics were then dried at 70 °C overnight. Polymers (0.5 g) were added into a beaker with 200 mL of DI water, after dissolving at 70 °C and the clean cotton fabrics were then added, before being ultrasonically incubated for 1 h. Afterwards, the fabric samples were pre-dried at 80 °C for 5 min, and cured at 160 °C for 5 min with a coating of the antimicrobial polymer. The silane-functionalized polyionene-coated fabrics were then washed with DI water to remove the unreacted polymers before being dried in an oven for 12 h at 80 °C.

2.4. Characterization of the polymers and the polymer-coated cotton fabrics

The polymers were characterized by gel permeation chromatography (GPC) for molecular weight and molecular weight distribution [25], by a Bruker Advance 400 NMR spectrometer for chemical structures [31], by thermogravimetric analysis (TGA) for thermal properties, and by field emission scanning electron microscopy (FE-SEM) combined with energy-dispersive X-ray spectroscopy (EDX) for surface morphology and chemical properties of the polymer-coated fabrics [6].

The water contact angle (CA) of the pristine and polymer-coated fabrics was measured by a contact angle analyzer at room temperature. Water droplets of 2.5 µL were placed on the surface of the fabrics, and the CA was recorded by video.

2.5. Evaluation of antimicrobial activity

2.5.1. Minimum inhibitory concentration (MIC), minimum bactericidal concentration (MBC) and minimum fungicidal concentration (MFC) of the polymers

The MICs of the polymers were determined against four clinically relevant microbial strains, namely *E. coli* and *P. aeruginosa* (Gram-negative), *S. aureus* (Gram-positive), and *C. albicans* (fungi) by a broth microdilution method [25].

MBC or MFC was defined as the lowest polymer concentration at which approximately 99.99% microbes were killed in the planktonic culture. Following the MIC experiment, 20 µL of microbial culture from each concentration was taken out from the 96 well plate and plated onto LB agar plates. The bacteria were incubated at 37 °C for 24 h, and the fungi were incubated at room temperature for 42 h. Samples from each test concentration were carried out in triplicates.

2.5.2. Killing efficiency of antimicrobial fabrics

Antimicrobial activity of the cotton fabrics was evaluated against *E. coli*, *S. aureus*, and *C. albicans* according to the protocol reported previously [7,32]. Bacterial and fungal cells were diluted to approximately 1-9 × 10^5 CFU mL^{-1} in PBS (70 mL), respectively. The polymer-treated cotton fabrics (0.75 g) and pristine cotton fabrics (0.75 g) were cut into pieces and added to the bacterial or fungal suspension, which were incubated at 37 °C for 24 h with shaking at 130 rpm. After that, 100 µL of culture medium was removed and serially diluted to the appropriate dilution before plating onto LB agar plates. The bacteria were incubated at 37 °C for 24 h, and the fungi were incubated at room temperature for 42 h. After that, the number of bacterial or fungal colonies on the plates were counted and killing rate was evaluated using the following equation: *Killing Efficiency* (%) = $(C_{control} - T_{sample})/C_{control} \times 100$, where $C_{control}$ is the number of bacterial or fungal colonies of the control sample; T_{sample} is the number of bacterial or fungal colonies of the treated cotton fabrics.

2.5.3. Bacterial and fungal killing kinetics

The bacteria and fungi were inoculated and prepared according to the same procedure as stated in Section 2.5.2. The coated and pristine
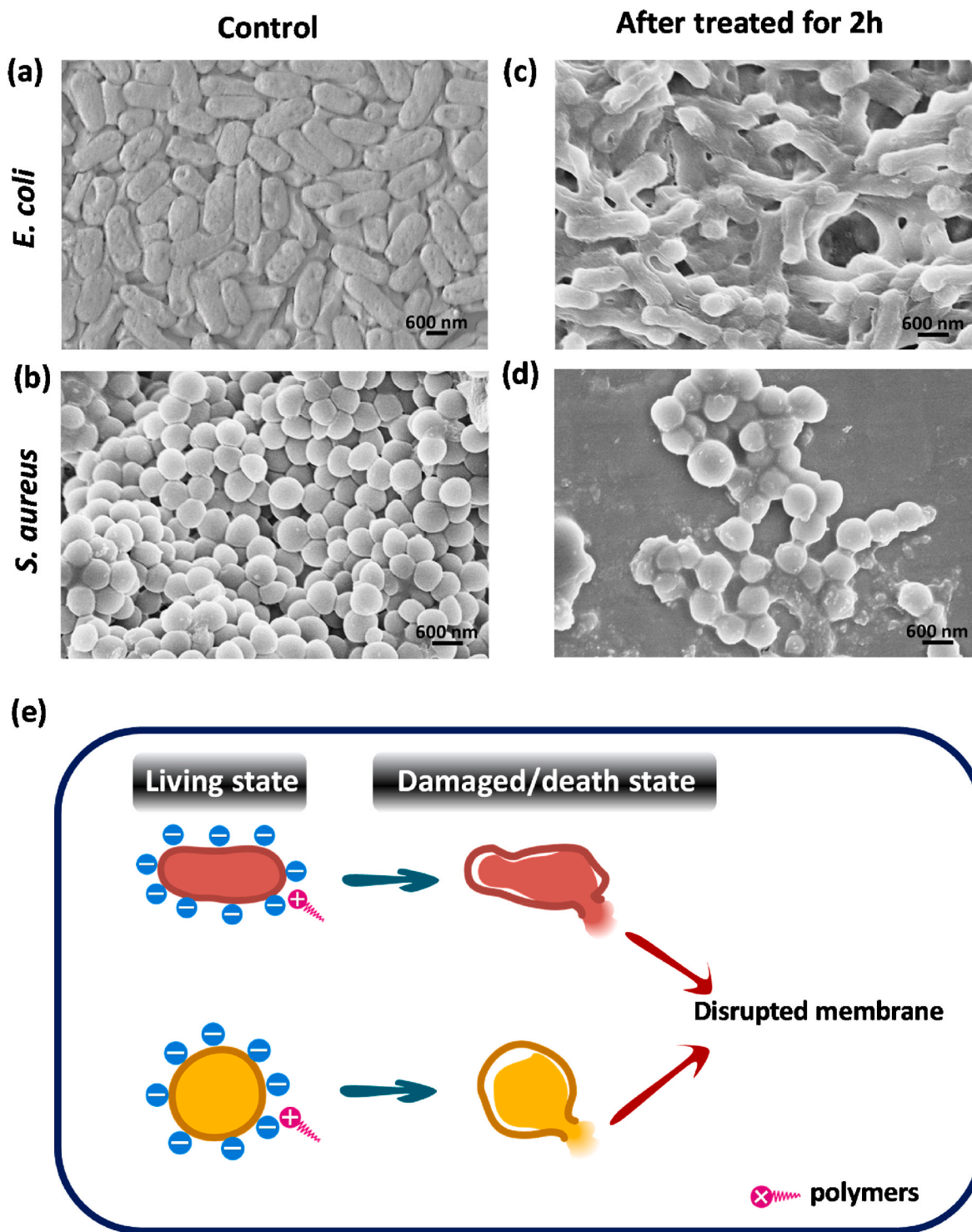
Fig. 1. FESEM images of bacteria before and after polymer treatment ((a) and (b) for control of *E. coli* and *S. aureus*, respectively, without any treatment; (c) and (d) for *E. coli* and *S. aureus* after treatment with **P1** at MBC for 2 h, respectively); (e) Antibacterial mode of action of the polymers.

cotton fabrics (0.75 g) were cut into pieces and added to the bacteria or fungi-containing PBS suspension (10^5 CFU mL^{-1}), and were incubated at 37 °C under constant shaking of 130 rpm. At regular time intervals (0 min, 15 min, 30 min, 60 min, 120 min, and 180 min), 100 μL of the bacterial samples was taken out for a series of 10-fold dilutions. The diluted bacterial suspension (20 μL) was plated onto a LB agar plate, and incubated for 24 h at 37 °C for bacteria, and for 42 h at room temperature for fungi. After incubation, the bacterial and fungal colonies were enumerated.

2.5.4. Zone of inhibition (ZOI) of antibacterial fabrics

ZOI is a parameter used to evaluate antimicrobial activity of materials [33,34]. The cotton fabrics were cut into circular samples with a radius of 1 cm. A 300 μL of bacterial suspension with 10^8 CFU mL^{-1} was plated onto the LB agar plates, and allowed to be absorbed for 10 min. The cotton fabric samples were then placed on the surface of the LB agar and incubated at 37 °C for 18 h. The pristine cotton fabric was used as control.
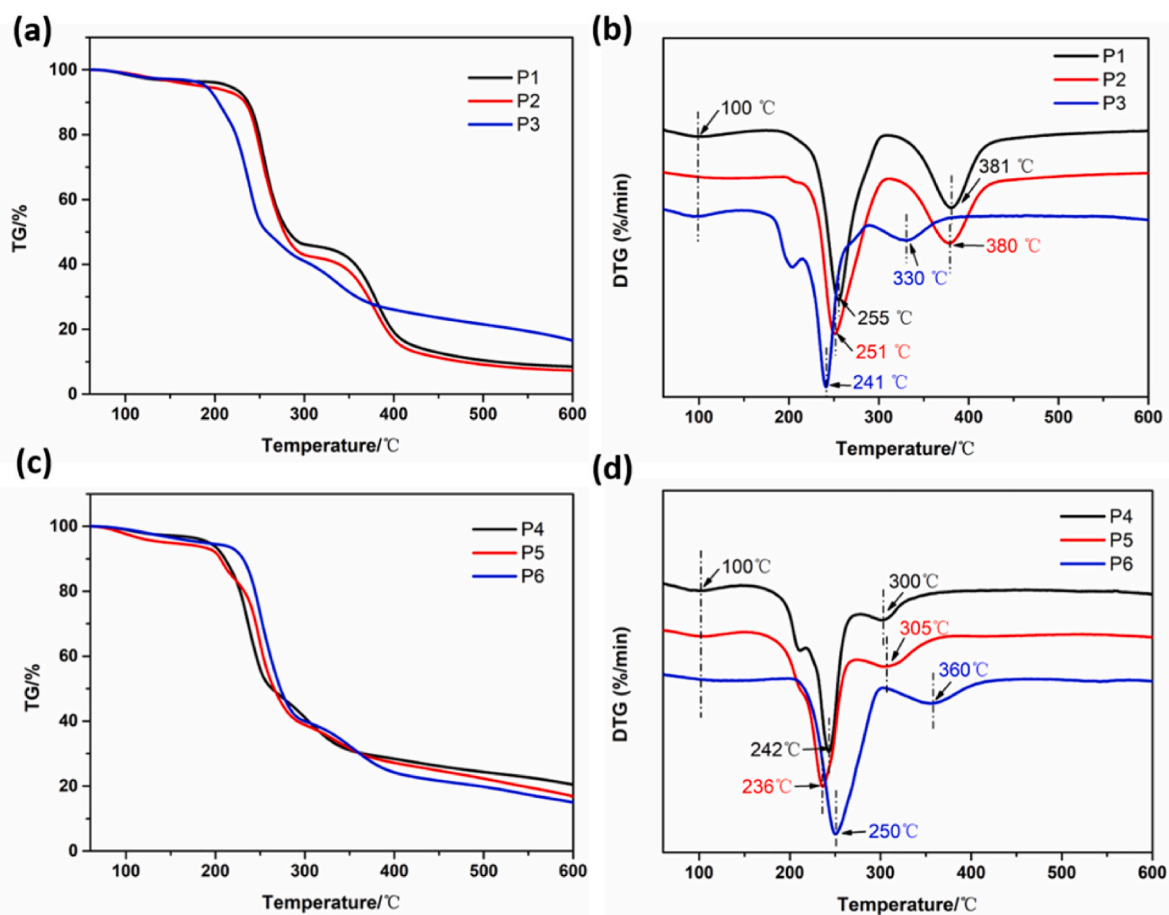
Fig. 2. Thermal properties of the silane-functionalized polyionenes. TGA curves of polymers: (a) P1, P2, and P3; (c) P4, P5, and P6. DTG curves of polymers: (b) P1, P2, and P3; (d) P4, P5, and P6.

2.5.5. Inhibition efficiency of bacterial adhesion of cotton fabrics

Bacteria adhesion of the antimicrobial polymer-treated cotton fabrics was studied as reported in the literature with slight modifications [35,36]. Both coated and pristine fabrics were immersed in 25 mL of bacterial suspension (*S. aureus*) with 10^7 CFU mL^{-1} and incubated under static conditions for 2 h at 37 °C. The fabrics were taken out and held vertically for 3 min to let remaining droplets slide away. Afterwards, the fabrics were placed in a tube containing 25 mL of fresh MHB and incubated for 24 h at 37 °C with shaking at 130 rpm. After the incubation, the samples were taken out and washed twice with 5 mL of sterile water to remove any unadhered bacteria. The samples were then put into a centrifuge tube containing 5 mL of PBS and sonicated for 2 min to remove the strongly adhered bacteria. The same procedure was performed five times and then mixed with the above PBS solution. Afterwards, 20 μL of this solution was plated onto the LB agar plate and further incubated at 37 °C for 24 h. After counting the number of colonies, the bacterial anti-adhesion rate was estimated as follows:

Inhibition efficiency of bacterial adhesion (%)

$$= \left(CFU_{control} mL^{-1} - CFU_{sample}\ mL^{-1}\right) / CFU_{control} mL^{-1} \times 100,$$

where $CFU_{control} mL^{-1}$ is the number of the viable bacteria for the pristine cotton fabrics, $CFU_{sample} mL^{-1}$ is the number of viable bacteria for the treated fabrics.

Bacterial adhesion on the fabrics was observed under FE-SEM after the above experiments. The resultant cotton fabrics were fixed with 2.5% glutaraldehyde solution for 1 h at 4 °C, and then washed twice with PBS. After that, the samples were dehydrated with a series of graded ethanol solution (50, 75, 90, and 100 wt %, for 15 min each), and then observed under FE-SEM after drying and treatment with platinum.

2.5.6. Antivirus assay using p22 bacteriophage

Briefly, 400 μL of p22 (~10^9 PFU mL^{-1}) suspension was spotted on the surface of polymer-treated and untreated cotton fabrics (50 × 50 mm^2) (samples were sterilized by autoclaving prior to starting the experiment). Then the samples were covered using PE cover slips (40 × 40 mm^2) to flatten the droplet (PE film cover slip sterilized using 75% ethanol and dried). Afterwards, the samples were incubated for 24 h at 25 °C at 90% humidity. After incubation, the cotton fabrics were resuspended in 10 mL of MHB medium to remove the adhered p22. The resuspended sample (100 μL) was then taken out and used for testing along with appropriate dilutions. After serial dilution, 60 μL of the resuspension was mixed with 60 μL of *Salmonella* suspension. Then, 6 mL of molten LB agar at 55 °C was added, and immediately poured onto a prewarmed LB agar plate, and allowed to solidify. Upon solidification of the agar, the plates were incubated at 37 °C overnight, before counting the plaques. The antivirus activity was calculated as follows: *Antiviral Activity* = $log10((U_{24h} - U_{0h}) - (T_{24h} - U_{0h}))$, where U_{24h} is the number of the plaques for the untreated cotton fabrics at 24 h, U_{0h} is the number of the plaques for the untreated cotton fabrics at 0 h, T_{24h} is the number of the plaques for the treated cotton fabrics at 24 h.

2.5.7. Antibacterial durability of the treated cotton fabrics

The washing procedure was performed according to the AATCC test method 61–2007 with some modifications. The fabrics were washed in DI water with 0.93% soap at 40 °C for 30 min, which was equivalent to five typical hand or home launderings. The samples were washed with different washing cycles, and then dried in ambient. The bacterial inhibition rate was measured after 10, 20, 30, 40 and 50 repetitive cycles.
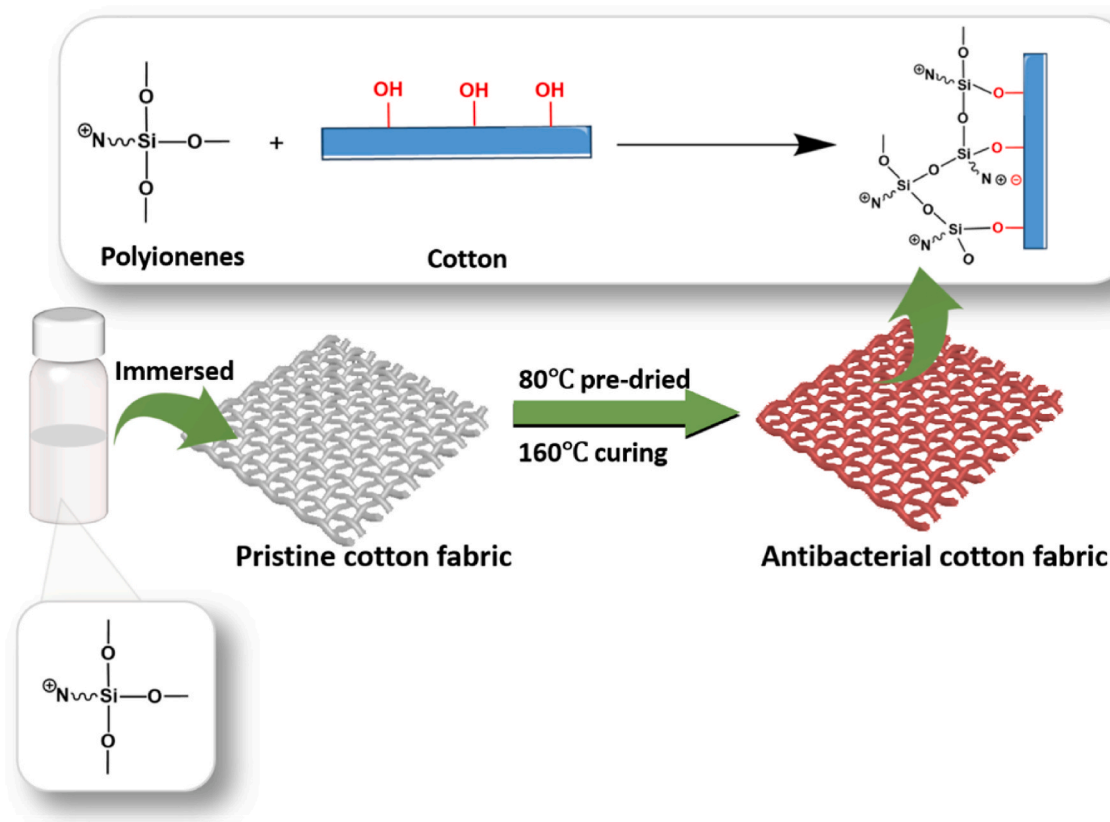
Fig. 3. Illustration of the coating process of cotton fabrics treated by the silane-functionalized polyionenes. The polymers were hydrolyzed first and then the hydrolytic polymers attached on the surface of cotton fabric by chemical conjugation and ionic interaction.

2.6. Cytotoxicity evaluation of the polymer-treated cotton fabrics

The cytotoxicity of the treated cotton fabrics was evaluated with alamar blue (ThermoFisher, U.S.A.) using L929 Fibroblast Cells. Both treated and untreated cotton fabrics (60 cm^2) were immersed into 20 mL of DMEM, and incubated at 37 °C, 5% CO_2 overnight. After that, the extracts of fabric samples were obtained. L929 cells were seeded into six-well plates at a density of 2×10^5 cells/mL (2 mL) and incubated at 37 °C, 5% CO_2 for 24 h. After incubation, the spent media was removed and replaced with aliquots of the respective sample extracts. Each sample was carried out in triplicates. The plates were incubated at 37 °C, 5% CO_2 for 48 h. Following that, the spent media was removed and 1 mL of fresh growth media comprising alamar blue (10% v/v) was added to each well and incubated for 3 h. The media with alamar blue from the various samples was then transferred into 96-well black plates with clear bottom (Greiner, Germany) and fluorescence was measured with excitation at 560 nm and emission at 590 nm using a microplate reader (TECAN, Switzerland).

2.7. Evaluation of skin irritation of the polymer-coated cotton fabrics in a mouse model

The animal skin irritation test was conducted according to ISO 10993-10: 2010: Biological evaluation of medical devices Part 10: Test for irritation and skin sensitization with some modifications. Female Balb/c mice (6–8 weeks old) were obtained from INVIVOS PTE. LTD. (Singapore). The mice were raised in a specific pathogen free animal lab. The animal study protocols were approved (IACUC No. 151096) by the Institutional Animal Care and Use Committee of Biological Resource Centre, Agency for Science, Technology and Research (A*STAR), Singapore. The fur on the back of BALB/c male mice was carefully clipped before directly applying either antibacterial or pristine cotton

fabric (1 × 1 cm^2) to the clipped area for five days. After five days, the cotton fabrics were removed and the skin area in contact with the fabrics was observed for erythema and edema. The skin area in contact with the fabrics was then excised, embedded in paraffin, sectioned and stained with Haematoxylin and Eosin (H&E) to observe for any inflammatory signals with a brightfield microscope (Leica DMi1).

3. Results and discussions

3.1. Polymer synthesis and characterization

To prepare potent antibacterial and antiviral polyionenes that can be coated onto hydroxyl-rich cotton fabrics, various silane-functionalized cationic polyionenes were synthesized. (3-Glycidyloxypropyl)trimethoxysilane (GPTMS), as a widely used coupling reagent, is a bifunctional organosilane bearing epoxy functional group. The methoxy groups attached on the silicon atom of GPTMS could be hydrolyzed in water to form silanol groups (Scheme 1), which can be further conjugated to the hydroxyl groups on the substrate surface via covalent bonds. To react with the epoxy group of GPTMS, (Scheme 1), 3,3-iminobis(*N,N*-dimethylpropylamine) was used to form DTA-TMS monomer *via* a ring-opening nucleophilic addition. Silane-functionalized polyionenes, **P1** and **P2**, were synthesized by varying the molar ratio of DTA-TMS, *N,N*, *N′,N′*-tetramethylethylenediamine (TMEDA) and α,α′-dichloro-p-xylene. The number of the silane groups in P1 and P2 is one and two, respectively. It is worth noting that the number of silane groups grafted to the polyionene was restricted to one or two groups to prevent the possible self-condensation of silanols when the silane-functionalized polyionenes were hydrolyzed and coated onto the surface of cotton fabrics [37,38]. The polymers were purified by extensive dialysis against DI water using dialysis membrane with a molecular weight cutoff (MWCO) of 1 kDa to further remove any trace small molecules left after the reaction,
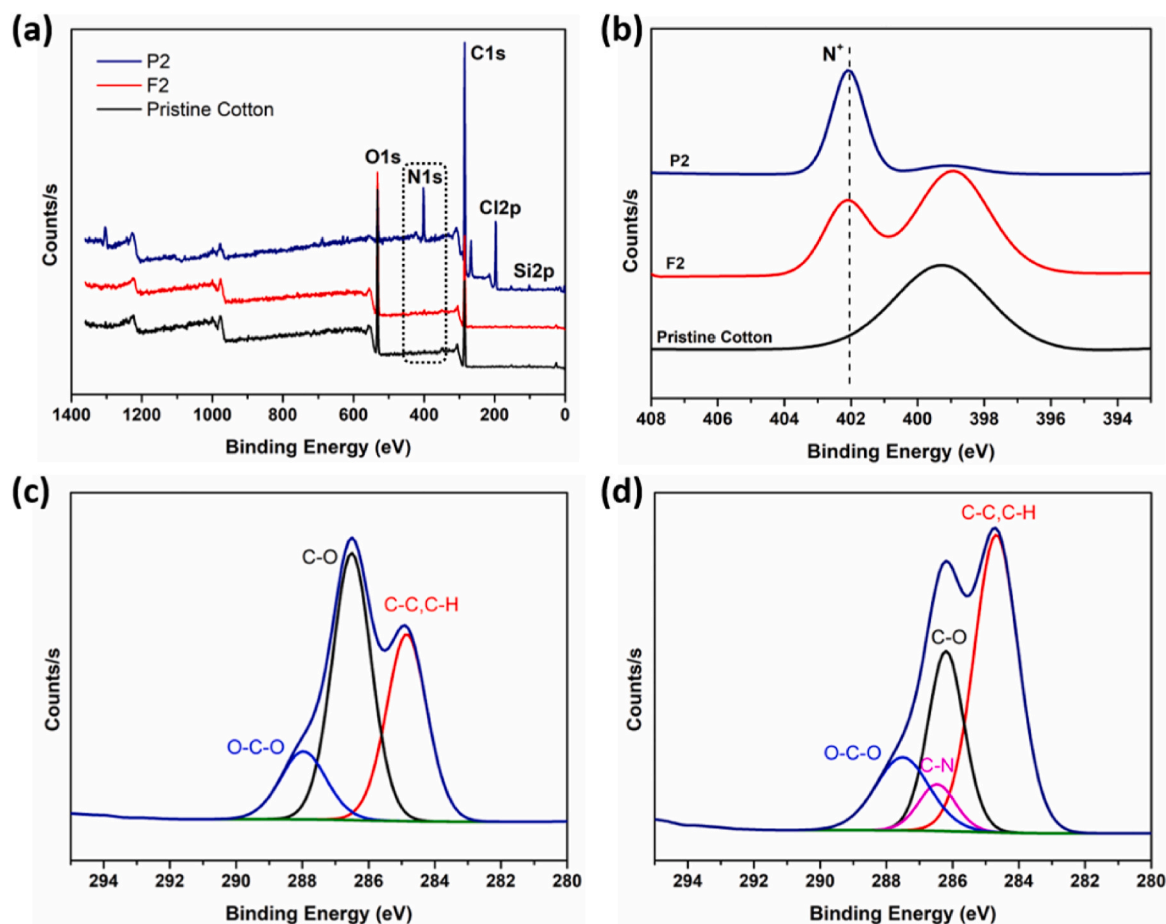
Fig. 4. (a) XPS spectra of **P2**, **F2** and pristine cotton fabric. (b) high-resolution N1s spectra of **P2**, **F2** and pristine cotton fabric. High-resolution C1s spectra of pristine cotton fabric (c) and **F2** (d).

especially ungrafted silane-containing monomers or oligomers, prior to GPC and ^{1}H NMR analyses. This was to achieve a relatively accurate number of silane groups grafted on the polymers. The unpurified polymers were directly coated onto the surface of the cotton fabric during the finishing process for easy preparation. GPC data showed that the elution curve of **P1** presented a single unimodal peak (Fig. S7) with an average molecular weight (Mn) of 4970 and the polydispersity (PDI) of 1.69 (Table 2). In contrast, a small shoulder peak present ahead of **P2** peak was observed in the GPC diagram (Fig. S8). This was probably due to the self-condensation between the silanol and hydroxyl groups derived from the nucleophilic addition of the silane-functionalized polyionene. The compositions of the polymers were estimated from ^{1}H NMR spectroscopy (Figs. S1 and 2) by quantitative comparisons between integral intensities of the peaks of the phenyl hydrogens from α,α′-dichloro-p-xylene at 7.72 ppm and the methylene protons attached to the silicon atom at 0.56 ppm, giving the number of silane grafted on the polyionene as one and two for **P1** and **P2**, respectively. Together with Mn values obtained from GPC diagrams, the degree of polymerization (DP) for the polyionenes was determined to be 16 for both **P1** and **P2** polymer (Table 2).

Similarly, 3-(triethoxysilyl)propyl isocyanate (IPTS) was also employed as the bifunctional coupling reagent for the monomer modification via addition reaction, giving rise to DTA-TES as another silane-conjugated monomer. Silane-functionalized polymer **P3** was obtained using the same polymerization protocol. A single unimodal peak was seen in the GPC diagram (Fig. S9) and the composition was estimated from ^{1}H NMR spectrum (Fig. S3) using the same calculation method for **P1** and **P2**, giving the number of silane grafted onto the polyionene as two. The molecular weight (Mn), PDI and DP values of the polyionene

P3 closely resembled those of **P1 and P2** in Table 2 due to their similar synthetic protocols.

To simplify the synthesis of silane-functionalized polyionenes on a large scale, (3-halopropyl)trimethoxysilanes (TMSPrX, halo represents chloride or bromide) was employed to prepare the silane-functionalized polyionenes via a one-pot quaternization reaction. As shown in Scheme 3, TMSPr-TA could be synthesized to completion by the quaternization of TMSPrX with TMEDA in excess. α,α′-Dichloro-p-xylene was then added to the above reaction solution to yield the silane-functionalized polyionene **P4** or **P5**. GPC data showed that the elution curve of each polymer presented a single unimodal peak (Figs. S10 and 11) with the molecular weight (Mn) of 3200 and 3,330, as well as the PDI value of 2.07 and 2.00, respectively. Similarly, the compositions of the polymers were estimated from ^{1}H NMR spectra (Figs. S4 and 5) using the same calculation method as above, giving the number of silane groups terminated on both polyionense chain approximately two. The molecular weight and DP values of **P4** and **P5** are nearly half of those of **P1** to **P3** due to the single tertiary amine of the silane-conjugated TMEDA which prevented chain propagation.

To enhance the polymerization and thereby enable the polyionene to achieve a high molecular weight, N,N,N',N'',N''-pentamethyldiethylenetriamine (PMDTA) was used to quaternize TMSPrBr to form a silane-grafted monomer (TMSPr-DTA) bearing two tertiary amines (Scheme 4). **P6** was obtained using the same polymerization protocol for **P1** to **P3**. A single unimodal peak was observed from the GPC diagram (Fig. S12) and the composition was estimated from ^{1}H NMR spectrum (Fig. S6) using the same calculation method with **P1** to **P5**. The number of silane groups grafted on the polyionene was determined to be approximately two. However, the molecular weight and DP
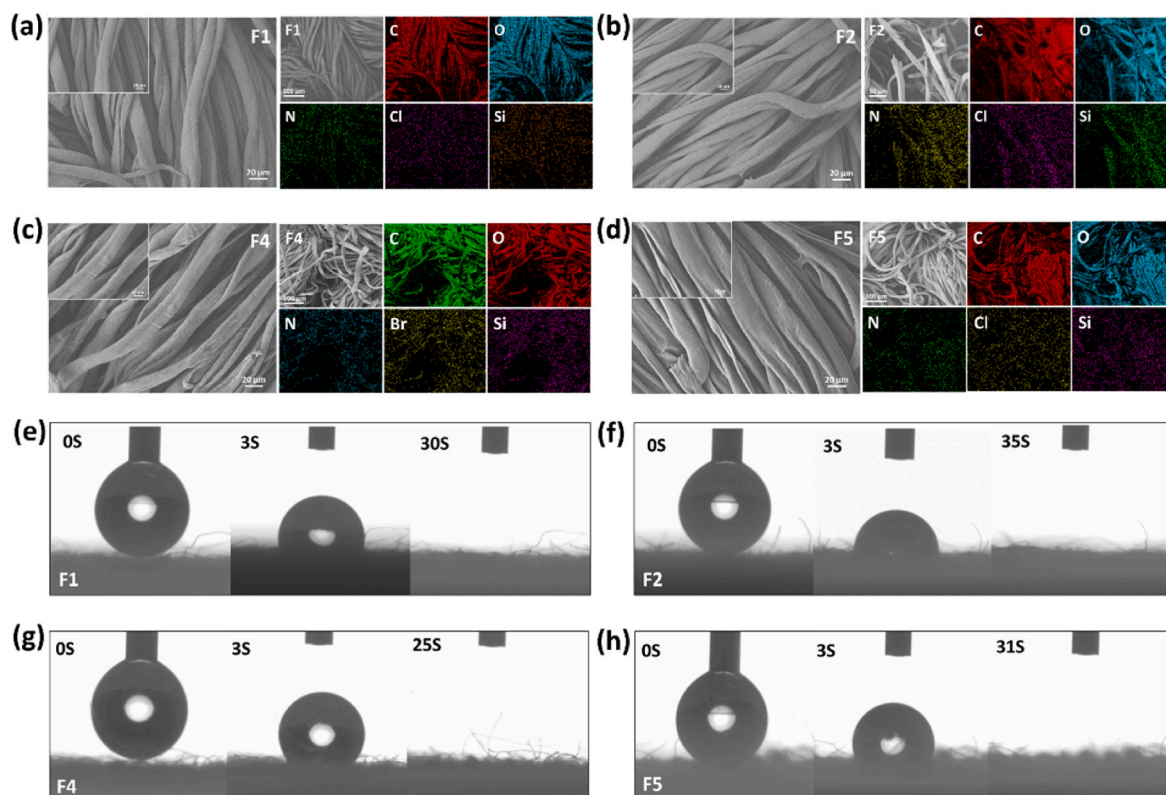
Fig. 5. FE-SEM images and EDX results of the antimicrobial cotton fabrics: F1 (a), F2 (b), F4 (c), and F5 (d). Water contact angle of the antimicrobial cotton fabrics: F1 (e), F2 (f), F4 (g), and F5 (h).

values of **P6** were observed to be slightly lower than those of **P4** and **P5.** This could probably because the two tertiary amines of TMSPr-DTA were sterically hindered by its quaternary amine group, leading to low chain propagation of the polyionene.

All the experimental conditions for synthesis of the above silane-functionalized polyionenes are summarized in Table 1, and their molecular characteristics data are summarized in Table 2.

3.2. Antimicrobial properties of the polymers

MIC and MBC/MFC of the polymers were evaluated to ascertain the antimicrobial activity of the polymers against bacteria and fungi. As shown in Tables 3 and 4, all the polymers demonstrated potent antimicrobial activity against *E. coli*, *S. aureus*, *P. aeruginosa* and *C. albicans*, with low MICs ranging within 3.91–15.63 μg/mL and low MBCs ranging from 3.91 to 31.25 μg/mL. It is interesting to note that the polymers exhibited high potency towards Gram-negative bacteria and inhibited the growth of both *E. coli* and *P. aeruginosa* at 7.81 μg/mL. Furthermore, the polymers also showed excellent activity towards fungi and the MICs of the polymers against *C. albicans* were between 3.91 and 15.63 μg/mL. In general, these results highlight the fact that the various factors such as silane coupling agent, tertiary amine used and DP of silane grafted does not affect the antimicrobial activity of these polymers significantly.

To understand the antibacterial mechanism of polymers, the morphological changes of bacteria after contact with polymers were investigated. As shown in Fig. 1, both *E. coli* and *S. aureus* bacteria which were not incubated with the polymer retained a smooth surface as well as their respective rodlike or spherical morphologies. This was in contrast to polymer-treated bacteria, which exhibited deformed surface membrane morphology. Moreover, lysis of the bacterial cells revealed numerous debris, which was indicative of substantial membrane damage and cytoplasmic leakage, and was consistent with the results of other

studies in the literature [6,39,40].

3.3. Thermal stability of the polymers

Thermogravimetric analysis (TGA) of the polymers was carried out to evaluate their thermal stability as the cationic quaternary ammonium groups might decompose at high temperature with substantial loss of antibacterial activity during the fabric coating process [41,42]. Particularly, the thermal stability of the silane-functionalized polyionenes was investigated by thermal gravimetry (TG) and derivative thermogravimetry (DTG) analysis (Fig. 2).

Thermal degradation of the polyionenes which occurred over several stages was measured as the loss of polymer mass over various temperatures. Fig. 2a and c showed the weight loss below 150 °C, which was attributed to the evaporation of absorbed water molecules. The polymers showed two main degradation steps in Fig. 2b and d, which could have been attributed to disintegration of the backbone of the polyionenes [43], and the low temperature stage may be due to the degradation of the oligomers, and the high temperature stage may stem from the degradation of the polymers. Overall, these results showed that the silane-functionalized polyionenes demonstrated good thermal stability below 180 °C. This was higher than the maximum temperature required for the fabrics finishing process (80–160 °C), thus further cementing the promising potential of silane-functionalized polyionenes as an antimicrobial coating for fabrics.

3.4. Preparation of antimicrobial cotton fabrics

The antimicrobial coating process of the cotton fabrics is shown in Fig. 3. Following the hydrolysis of trialkylsilane, the newly introduced silanol groups in the polyionene backbone were able to react with the hydroxyl groups present on the surface of the cotton fabric. This resulted
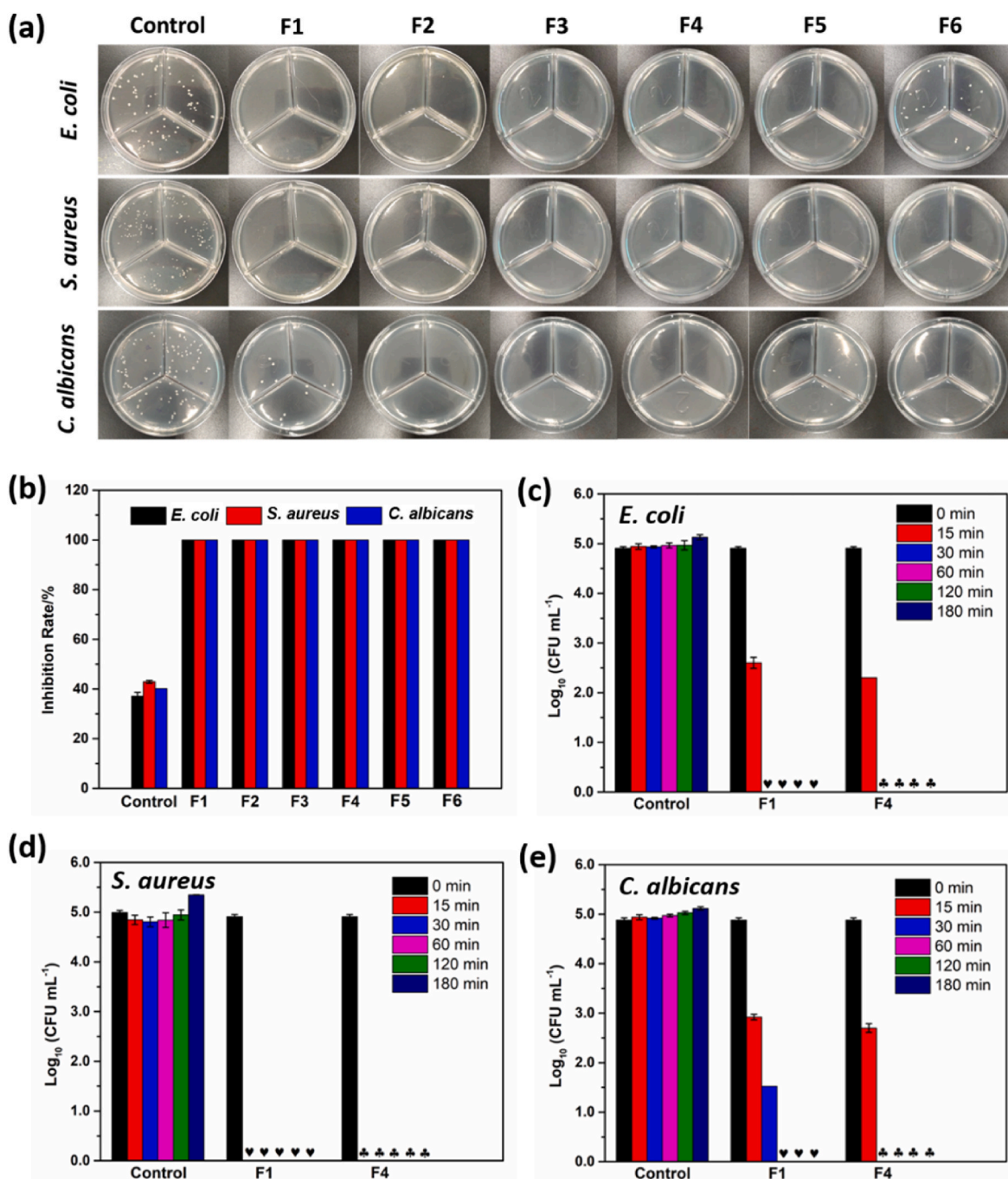
Fig. 6. (a) Antibacterial properties of the treated fabrics by plate counting method, raw cotton as control sample. (b) Inhibition rate of the treated cotton fabrics. Killing kinetics of F1 and F4 on *E. coli* (c), *S. aureus* (d), and *C. albicans* (e) (♥♣ denote no colonies were observed).

in the formation of covalent bonds between the antimicrobial polyionenes and cotton fabrics during the curing process, thus transforming the cotton fabrics into antimicrobial textiles. In addition, ionic interactions were also formed between the polyionenes and cotton surface as a result of the attraction between the cationic charge on the polymers and the negative charge on the surface of the cotton fibers. The success of the curing process was evidenced by X-ray photoelectron spectroscopy (XPS). Compared to the pristine cotton fabrics in Fig. 4a and b, the N1s peak at 402.5 eV that was assigned to the positively charged nitrogen (N^+) was found in the XPS spectra of the finished cotton fabrics with **P2** [8,28]. Additionally, in Fig. 4c and d, for the pristine cotton fabric and **F2**, the C1s peaks at 284.4 eV, 286 eV, and 287 eV could be attributed to the C–C and C–H bonds, C–O bund, and O–C–O bond,

respectively [44]. Notably, the C1s peak at about 286.5 eV can be found in the Fig. 4d, corresponding to the C–N group of **P2**, in the high-resolution C1 spectrum of **F2** [8]. These results indicate that **P2** was successfully attached to cotton fabrics through chemical bonding.

Field emission scanning electron microscopy (FE-SEM) and SEM with energy dispersive X-Ray analysis (SEM-EDX) mapping demonstrated that the surface elements (C, O, N, Cl/Br, and Si) were distributed uniformly on the treated fabric surface (Fig. 5a–d). Moreover, FE-SEM images showed that the fibers of the polymer-treated cotton fabrics remained intact during the coating process. Further investigation was undertaken by measuring the water contact angles (WCAs) on the treated cotton fabrics. As shown in the Figure S13, due to the rough, porous, and naturally hydrophilic properties of the pristine cotton
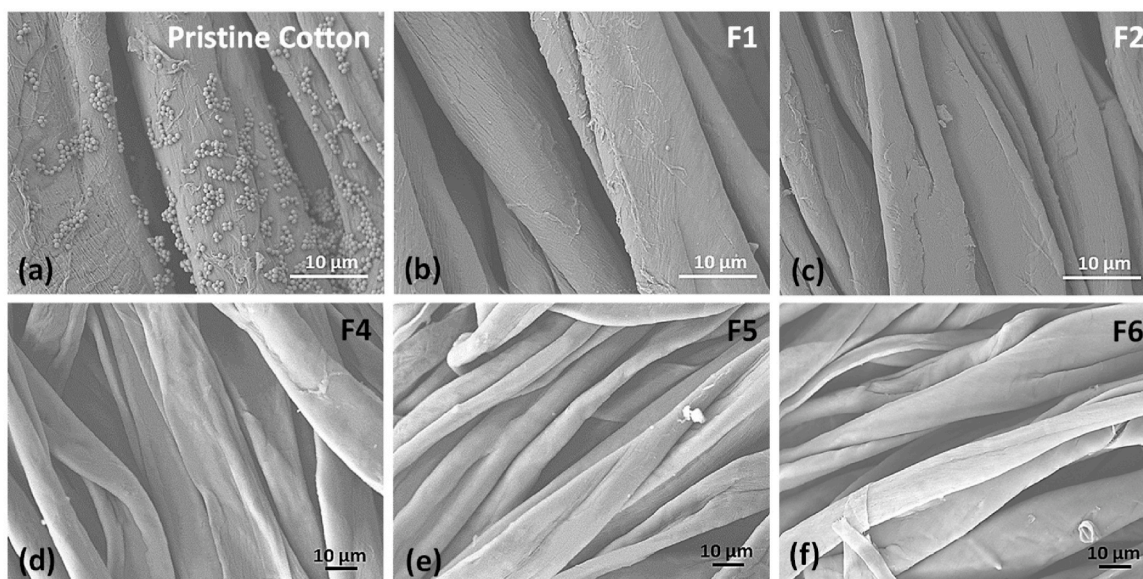
Fig. 7. FE-SEM images of the adhered bacteria on the pristine cotton and polymer-coated cotton fabrics. (a) pristine cotton, (b) F1, (c) F2, (d) F4, (e) F5, and (f) F6.
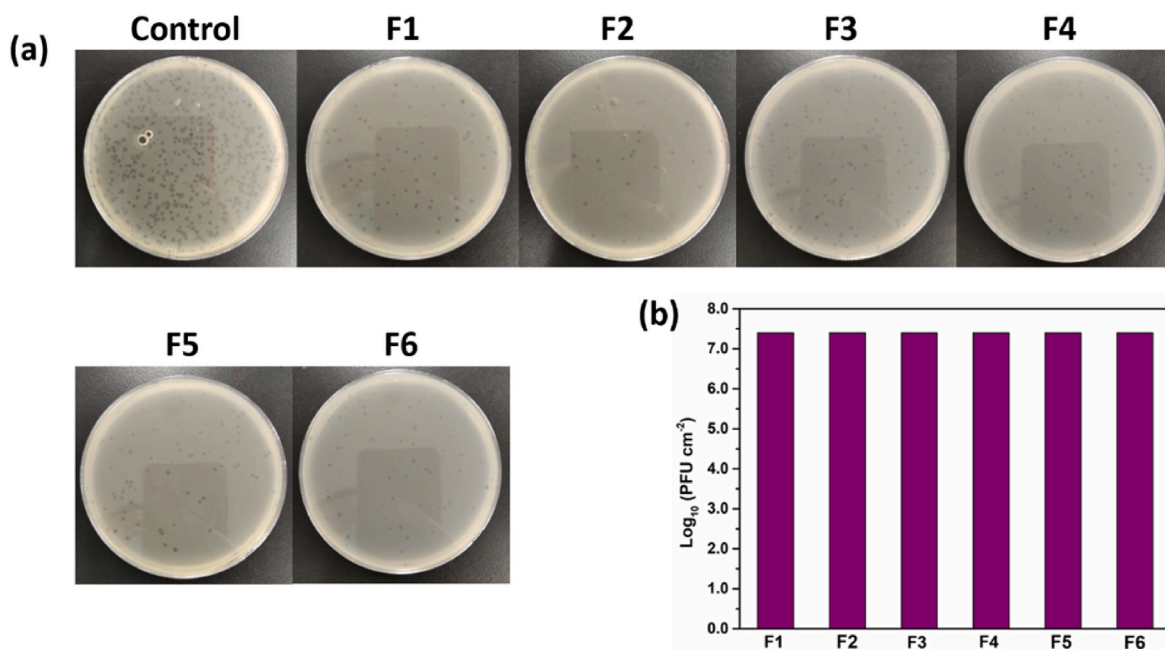

Fig. 8. (a) Antiviral test of the treated cotton fabrics for p22. (b) PFU reduction count of the treated cotton fabrics for p22 (The error bar is too small to display).

fabric, the water droplets could spread at an extremely fast speed on the fabric surface and the WCAs reached 0° immediately. By comparison, as exhibited in Fig. 5e–h, the WCAs of the treated cotton fabrics reached 0° after more than 25 s. It was deduced that the coated polymers could change the surface properties of the fabric, thereby leading to a change in the contact angle. The presence of aryl groups in the polymer backbone and silicon-oxygen bond in the polymer side chain could have reduced the hydrophilicity of the fabrics.

3.5. Activity of polyionene-coated cotton fabrics against bacteria, fungi and virus

Antimicrobial activity of the silane-treated cotton fabrics upon contact with *E. coli*, *S. aureus* and *C. albicans* was evaluated. It was found

that the polyionene-coated fabrics were able to achieve a 5 log CFU reduction for *E. coli*, *S. aureus* and *C. albicans*, which corresponded to a killing efficiency of 99.999% (Fig. 6a and b). This was in line with the minimal number of bacterial or fungal colonies observed on the plates as compared to the significant microbial growth of the controls. These results thus demonstrate the highly potent antimicrobial activity of the polyionene-coated cotton fabrics. The killing kinetics of the treated cotton fabrics were further evaluated on *E. coli*, *S. aureus* and *C. albicans*. Herein, the fabrics coated by **P**1 and **P**4 were used as examples. As illustrated in Fig. 6c and e, the P1 and P4-treated cotton fabrics induced a greater than 2-log reduction in the number of viable *E. coli* and *C. albicans* colonies (>99% killing efficiency) within 5 min, and eradicated all the microbial cells in 15 min, indicating a rapid bactericidal/ fungicidal mechanism. In the case of *S. aureus*, the killing efficiency was
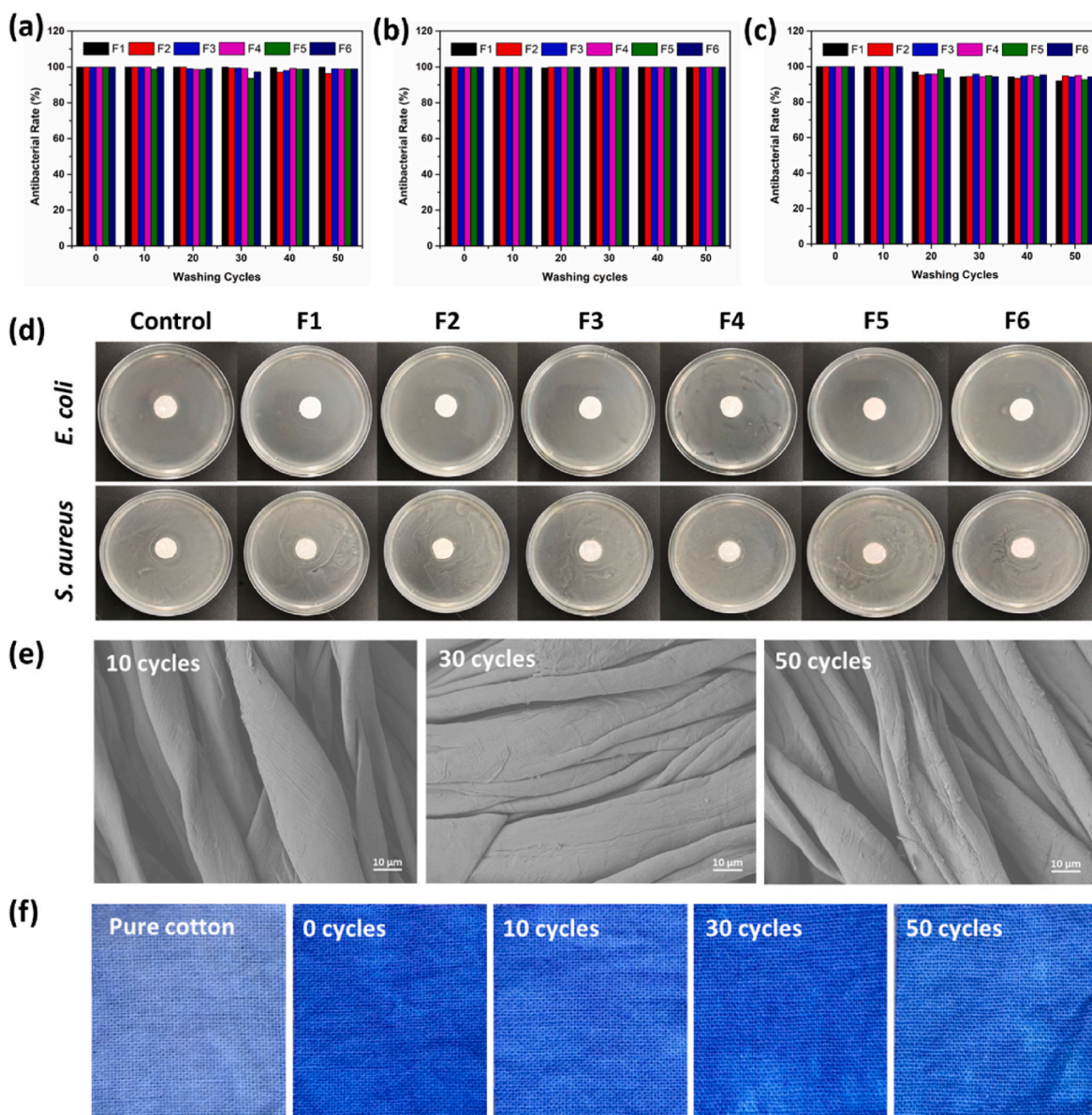
Fig. 9. Antimicrobial activity of the polyionene-coated cotton fabrics after washing. (*E. coli* (a), *S. aureus* (b), and *C. albicans* (c)). (d) ZOI of the coated cotton fabrics on *E. coli* and *S. aureus*. (e) FE-SEM of the F1 after 10, 30 and 50 cycles of washing. (f) Analysis of quaternary ammonium cations remained on F1 using bromophenol blue after different washing cycles. (For interpretation of the references to color in this figure legend, the reader is referred to the Web version of this article.)

almost 100% at 5 min (Fig. 6d). This might be due to the lack of the outer membrane, which makes Gram-positive bacteria more susceptible to the polyionene-coated fabric treatment as compared to Gram-negative bacteria [45,46].

Bacterial adhesion to the fabric surface was also observed by FE-SEM. As shown in Fig. 7, the polyionene-coated fabrics demonstrated considerable reduction in bacterial adhesion as compared to the pristine cotton fabrics. Currently, the strategies commonly employed to reduce bacterial adhesion to surfaces involve either the repulsion or killing of the bacteria in contact with the surface. Bactericidal effects were achieved through release- or contact-killing methods [45,47–50]. In our study, the bactericidal effects of the polyionene-coated fabrics were achieved via contact killing as a result of covalent bonds formed between the polyionenes and cotton fabrics.

As a result of the heightened threat of viral outbreaks to public health in recent years, the ability of cotton fabrics to kill or inactivate viruses has become an increasingly important attribute. To assess the antiviral potential of the polyionene-treated cotton fabrics, the anti-viral activity

of the polyionene-coated fabrics was evaluated using p22 bacteriophage as a model virus by salmonella-based plating assay. As observed in Fig. 8a and b, the polyionene-coated cotton fabrics achieved rapid and effective killing of the p22 phages as evidenced by the 7-log PFU (plaque-forming units) reduction. This contrasted with the controls in which the harvested phages were able to proliferate rapidly on the *Salmonella*-based culture media. These results further highlight the excellent antiviral activity of the polyionene-coated fabrics and pave the way for further investigation of the anti-viral activity of these polymers against other viral species for future work.

3.6. Laundering durability of the antimicrobial cotton fabrics

The antimicrobial durability of the polyionene-coated cotton fabrics was assessed by analyzing the antimicrobial activity of these fabrics when subjected to different numbers of wash cycles. As shown in Fig. 9a–c, the antimicrobial activity of the coated cotton fabrics against *E. coli*, *S. aureus* and *C. albicans* did not show significant change even
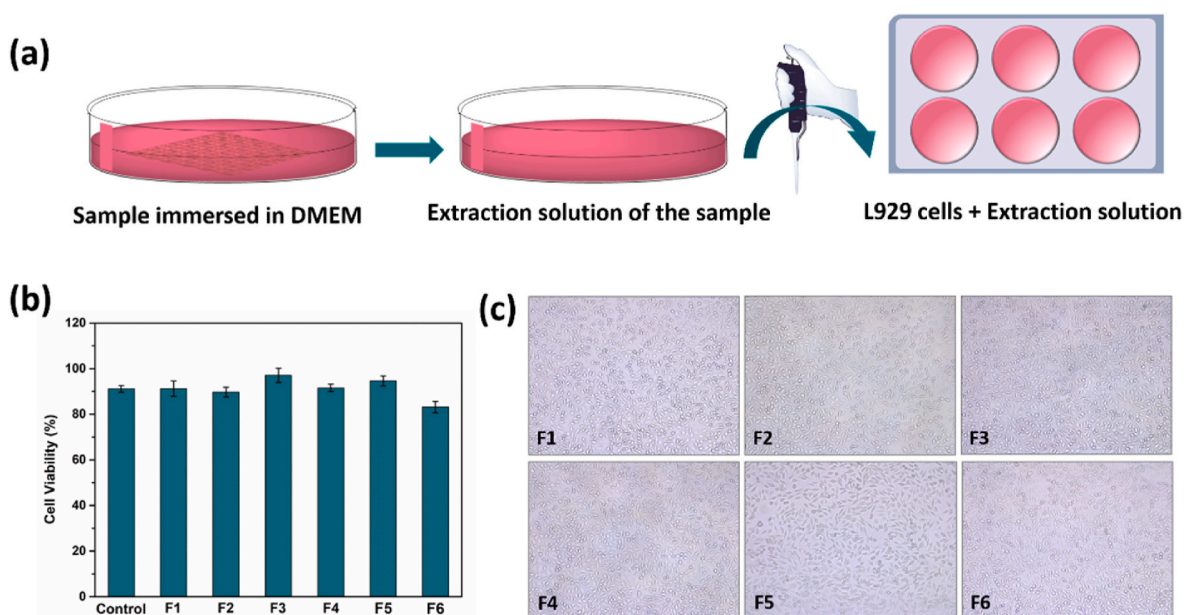
Fig. 10. *In vitro* cytotoxicity studies: (a) Schematic illustration of cytotoxicity evaluation. (b) Viability of L929 cells cultured with the extraction solution of the polymer-coated cotton fabrics. (c) Representative microscopy images of L929 cultured with the polymer-coated fabrics (F1–F6).

with high number of washes, up to 50 times. This thus demonstrated the durable retention of antibacterial activity of the polyionene-coated fabrics even when the coated fabrics were subjected to high stress activities such as detergent washing.

The excellent retention of antibacterial activity of these polyionene-coated cotton fabrics could be attributed to the silane groups introduced into the polyionene backbone. These groups covalently reacted with the hydroxyl groups on the fabric surface, thus preventing the dissolution and subsequent loss of these polymers in water when subjected to increasing numbers of wash cycles. Additional evidence further lends credence to the high retention of antibacterial activity of these polyionene-coated fabrics. These include no polyionene leakage as determined by the ZOI tests (0 mm, Fig. 9d) using *E. coli* and *S. aureus* and negligible alteration of surface topography of the coated fabrics after different numbers of wash cycles (Fig. 9e).

An additional qualitative test involving the use of bromophenol blue to form blue complexes with quaternary ammonium cations was used to determine the amount of quaternary ammonium polymers left on the coated cotton fabrics following the different numbers of wash cycles. As shown in Fig. 9f, the deep blue coloration demonstrated the presence of the quaternary ammonium polymers on the cotton fabrics even after 50 washes. This was in contrast to the pristine cotton fabrics which only showed a light blue color, which was indicative of only bromophenol blue.

3.7. Biocompatibility of the treated cotton fabrics

3.7.1. In vitro cytotoxicity studies

Cytotoxicity of the polyionene-coated fabrics was determined in L929 cells using the alamar blue cell viability assay. Incubation of the polymer-coated fabrics with the cells demonstrated minimal cytotoxicity as evidenced by the high cell viability of >85%, which was measured post 48 h of incubation (Fig. 10b). A similar explanation underlying the long retention of antimicrobial activity of the coated fabrics could also be used to explain the low cytotoxicity of the polymer-coated fabrics. The technique used to covalently graft the polymer onto the fabric surface ensured that the polymer did not leach out into the culture media over time. This explanation was further supported when the cells were treated for 48 h with previously prepared leachate (polymer-coated fabrics immersed in DMEM). As seen in Fig. 10c, the cells were

able to proliferate well and no abnormal cellular morphology was observed.

3.7.2. Evaluation of skin irritation

In accordance with safety standards for antibacterial textiles, evaluation of skin irritation must be carried out in pre-clinical models. To evaluate the safety of the polyionene-coated fabrics, both the pristine and treated cotton fabrics were applied directly onto the back of mice. After five days, neither erythema nor edema was observed on the skin as shown in Fig. 11b and c. Staining of the paraffin-embedded skin tissue which was in contact with the fabrics with haematoxylin and eosin (H&E) did not reveal any obvious histopathological abnormalities (Fig. 11d and e). These results thus revealed that the polymer-coated cotton fabrics were compatible with the skin.

4. Conclusion

Several series of silane-functionalized polyionenes have been designed, synthesized and applied onto cotton fabrics through chemical conjugation to render antimicrobial and antiviral activities. Assessment of antimicrobial activity of the polymers revealed high potency with low MIC and MBC/MFC values against *E. coli*, *S. aureus*, *P. aeruginosa*, and *C. albicans* caused by cell membrane disruption. More importantly, the polyionene-coated fabrics exhibited strong antiviral activity. The excellent retention of antimicrobial activity even after repeated washes, prevention of bacterial adhesion, potent antiviral activity, good cytocompatibility and skin compatibility of these polyionene-coated fabrics further highlight their promising potential as coating materials for textiles and other applications to prevent microbial and viral infections.
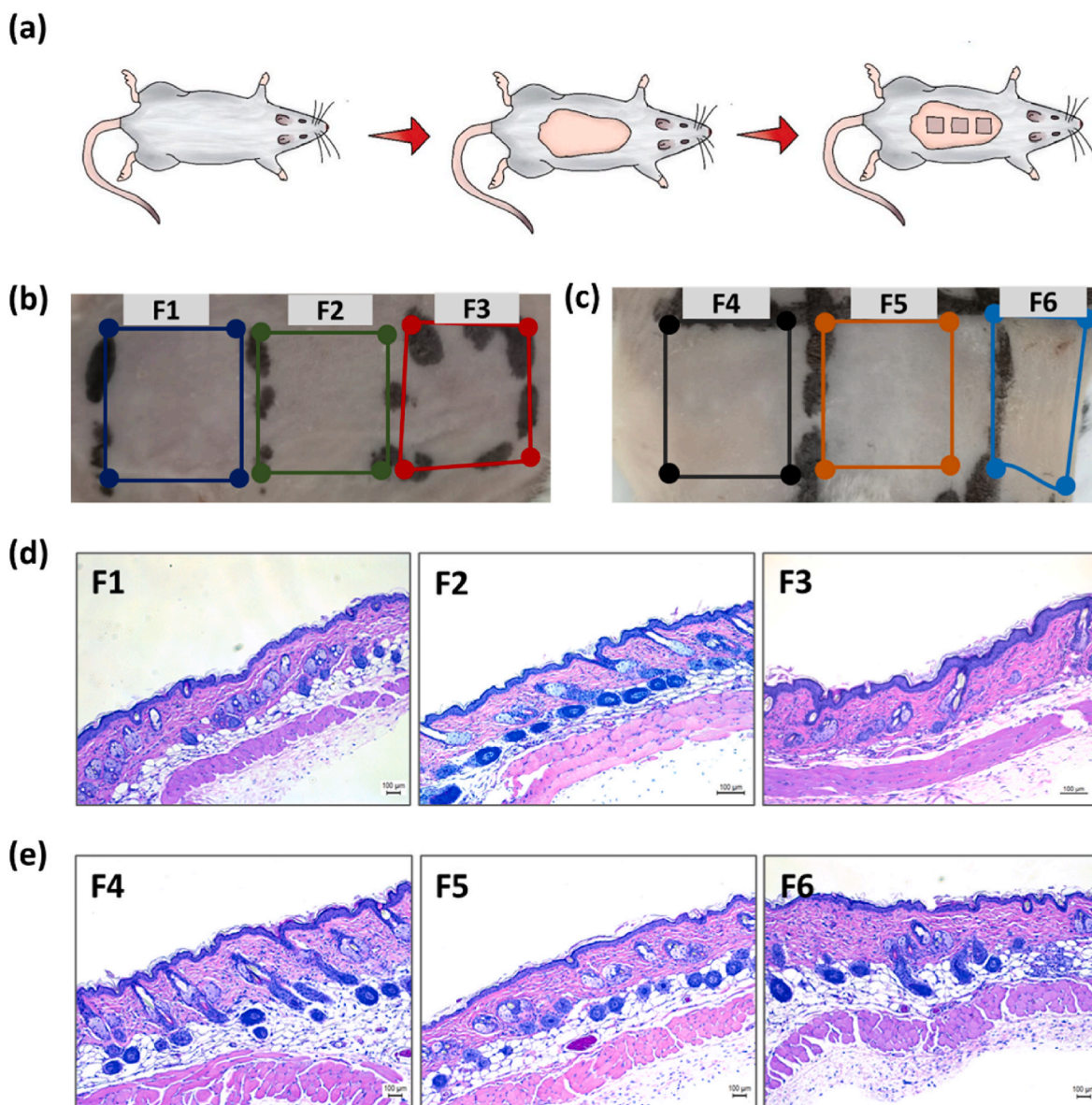
Data availability

The raw data are available from the corresponding author and the authors upon request.

Credit author statement

Qiaohua Qiu: Conceptualization, Methodology, Investigation (polymer coating, and all other studies), Visualization, Writing- Original draft preparation. Chuan Yang: Conceptualization, Methodology,

Fig. 11. Skin irritation evaluation: (a) Schematic illustration of skin irritation evaluation. (b) and (c) The images showing mouse back contacting with the polymer-coated cotton fabrics at 5 days. (d) and (e) H&E staining images of skin that was in contact with the polymer-coated fabrics at 5 days.

Investigation (polymer synthesis), Writing- Original draft preparation. Yanming Wang: Methodology, Investigation (animal study). Cherylette Anne Alexander: Writing- Reviewing and Editing. Guangshun Yi: Investigation (SEM), Writing- Reviewing and Editing. Yugen Zhang: Investigation (SEM), Writing- Reviewing and Editing. Xiaohong Qin: Funding acquisition, Writing- Reviewing and Editing. Yi Yan Yang: Conceptualization, Supervision, Writing- Reviewing and Editing, Funding acquisition.

Declaration of competing interest

The authors declare that they have no known competing financial interests or personal relationships that could have appeared to influence the work reported in this paper.

Acknowledgments

Appendix A. Supplementary data

Supplementary data to this article can be found online at https://doi.org/10.1016/j.biomaterials.2022.121470.

References

[1] M.E. Halloran, I.M. Longini, Emerging, evolving, and established infectious diseases and interventions, Science 345 (2014) 1292–1294.

[2] E.C. Holmes, G. Dudas, A. Rambaut, K.G. Andersen, The evolution of Ebola virus: insights from the 2013-2016 epidemic, Nature 538 (2016) 193–200.

[3] J.J. Zhang, M. Litvinova, Y.X. Liang, Y. Wang, W. Wang, S.L. Zhao, et al., Changes incontact patterns shape the dynamics of the COVID-19 outbreak in China, Science 368 (2020) 1481–1486.

[4] Q. Li, X.H. Guan, P. Wu, X.Y. Wang, L. Zhou, Y.Q. Tong, et al., Early transmission dynamics in Wuhan, China, of novel Coronavirus-infected pneumonia, N. Engl. J. Med. 382 (2020) 1199–1207.

[5] Y. Si, Z. Zhang, W.R. Wu, Q.X. Fu, K. Huang, N. Nitin, et al., Daylight-driven rechargeable antibacterial and antiviral nanofibrous membranes for bioprotective applications, Sci. Adv. 4 (2018) 12.

[6] J. Lin, X.Y. Chen, C.Y. Chen, J.T. Hu, Z. Guo, Durably antibacterial and bacterially anti-adhesive cotton fabrics coated by cationic fluorinated polymers, ACS Appl. Mater. Interfaces 10 (2018) 6124–6136.

[7] Q.H. Qiu, S.Y. Chen, Y.P. Li, Y. Yang, H.N. Zhang, Z.Z. Quan, et al., Functional nanofibers embedded into textiles for durable antibacterial properties, Chem. Eng. J. 384 (2020) 123241.

[8] S.G. Chen, S.J. Chen, S. Jiang, M.L. Xiong, J.X. Luo, J.N. Tang, et al., Environmentally friendly antibacterial cotton textiles finished with siloxane sulfopropylbetaine, ACS Appl. Mater. Interfaces 3 (2011) 1154–1162.

[9] D.S. Morais, R.M. Guedes, M.A. Lopes, Antimicrobial approaches for textiles: from research to market, Materials 9 (2016) 498.

[10] K.K. Goli, N. Gera, X. Liu, B.M. Rao, O.J. Rojas, J. Genzer, Generation and properties of antibacterial coatings based on electrostatic attachment of silver nanoparticles to protein-coated polypropylene fibers, ACS Appl. Mater. Interfaces 5 (2013) 5298–5306.

[11] F.Y. Fu, L.Y. Li, L.J. Liu, J. Cai, Y.P. Zhang, J.P. Zhou, et al., Construction of cellulose based ZnO nanocomposite films with antibacterial properties through one-step coagulation, ACS Appl. Mater. Interfaces 7 (2015) 2597–2606.

[12] Y. Xu, W. Wen, J.M. Wu, Titania nanowires functionalized polyester fabrics with enhanced photocatalytic and antibacterial performances, J. Hazard Mater. 343 (2018) 285–297.

[13] J. Ren, W.Z. Wang, S.M. Sun, L. Zhang, L. Wang, J. Chang, Crystallography facet-dependent antibacterial activity: the case of Cu2O, Ind. Eng. Chem. Res. 50 (2011) 10366–10369.

[14] H.R. Tian, Y.S. Zhai, C. Xu, J. Liang, Durable antibacterial cotton fabrics containing stable acyclic N-halamine groups, Ind. Eng. Chem. Res. 56 (2017) 7902–7909.

[15] D.H. Xu, S.J. Wang, J.W. Hu, Y. Liu, Z.M. Jiang, P. Zhu, Enhancing antibacterial and flame-retardant performance of cotton fabric with an iminodiacetic acid-containing N-halamine, Cellulose 28 (2021) 1–13.

[16] Z.L. Li, J. Chen, W. Cao, D.F. Wei, A.N. Zheng, Y. Guan, Permanent antimicrobial cotton fabrics obtained by surface treatment with modified guanidine, Carbohydr. Polym. 180 (2018) 192–199.

[17] L.J. Sun, S.S. Yang, X.R. Qian, X.H. An, High-efficacy and long term antibacterial cellulose material: anchored guanidine polymer via double "click chemistry, Cellulose 27 (2020) 8799–8812.

[18] C.K. Kang, S.S. Kim, S. Kim, J. Lee, J.-H. Lee, C. Roh, et al., Antibacterial cotton fibers treated with silver nanoparticles and quaternary ammonium salts, Carbohydr. Polym. 151 (2016) 1012–1018.

[19] W. Tian, Y. Hu, W. Wang, D. Yu, Synthesis of a gemini quaternary ammonium salt and its reaction with wool fabric using click chemistry, RSC Adv. 5 (2015) 91932–91936.

[20] F. Qi, Y.X. Qian, N. Shao, R.Y. Zhou, S. Zhang, Z.Y. Lu, et al., Practical preparation of infection-resistant biomedical surfaces from antimicrobial β-peptide polymers, ACS Appl. Mater. Interfaces 11 (2019) 18907–18913.

[21] Z.Y. Lu, Y.M. Wu, Z.H. Cong, Y.X. Qian, X. Wu, N. Shao, et al., Effective and biocompatible antibacterial surfaces via facile synthesis and surface modification of peptide polymers, Bioact. Mater. 6 (2021) 4531–4541.

[22] Fitzpatrick RJ, Klinger JD, Shackett KK. Ionene polymers and their use as antimicrobial agents: U.S. Patent 6,955,806. 2005-10-18.

[23] S.R. Williams, T.E. Long, Recent advances in the synthesis and structure-property relationships of ammonium ionenes, Prog. Polym. Sci. 34 (2009) 762–782.

[24] T. Narita, R. Ohtakeyama, M. Nishino, J.P. Gong, Y. Osada, Effects of charge density and hydrophobicity of ionene polymer on cell binding and viability, Colloid Polym. Sci. 278 (2000) 884–887.

[25] S.Q. Liu, R.J. Ono, H. Wu, J.Y. Teo, Z.C. Liang, K.J. Xu, et al., Highly potent antimicrobial polyionenes with rapid killing kinetics, skin biocompatibility and invivo bactericidal activity, Biomaterials 127 (2017) 36–48.

[26] S. Venkataraman, J.P.K. Tan, S.T. Chong, C.Y.H. Chu, E.A. Wilianto, C.X. Cheng, et al., Identification of structural attributes contributing to the potency and selectivity of antimicrobial polyionenes: amides are better than esters, Biomacromolecules 20 (2019) 2737–2742.

[27] S. Bernardi, M. Renault, A. Malabirade, N. Debou, J. Leroy, J.M. Herry, et al., Robust grafting of polyionenes: new potent and versatile antimicrobial surfaces, Macromol. Biosci. (2020) 20.

[28] S.B. Zhang, X.H. Yang, B. Tang, L.J. Yuan, K. Wang, X.Y. Liu, et al., New insights into synergistic antimicrobial and antifouling cotton fabrics via dually finished with quaternary ammonium salt and zwitterionic sulfobetaine, Chem. Eng. J. 336 (2018) 123–132.

[29] J.W. Gu, L.J. Yuan, Z. Zhang, X.H. Yang, J.X. Luo, Z.F. Gui, et al., Non-leaching bactericidal cotton fabrics with well-preserved physical properties, no skin irritation and no toxicity, Cellulose 25 (2018) 5415–5426.

[30] J.D. Bos, M.M. Meinardi, The 500 Dalton rule for the skin penetration of chemical compounds and drugs, Exp. Dermatol. 9 (2000) 165–169.

[31] X. Ding, C. Yang, T.P. Lim, Y.H. Li, A.C. Engler, J.L. Hedrick, et al., Antibacterial and antifouling catheter coatings using surface grafted PEG-b-cationic polycarbonate diblock copolymers, Biomaterials 33 (2012) 6593–6603.

[32] H. Han, J. Zhu, D.Q. Wu, F.X. Li, X.L. Wang, J.Y. Yu, et al., Inherent guanidine nanogels with durable antibacterial and bacterially antiadhesive properties, Adv. Funct. Mater. 29 (2019).

[33] J. Lin, X.Y. Chen, C.Y. Chen, J.T. Hu, C.L. Zhou, X.F. Cai, et al., Durably antibacterial and bacterially antiadhesive cotton fabrics coated by cationic fluorinated polymers, ACS Appl. Mater. Interfaces 10 (2018) 6124–6136.

[34] X.X. Chen, F. Fang, X. Zhang, Y.Y. Wang, L. Chen, et al., Flame-retardant, electrically conductive and antimicrobial multifunctional coating on cotton fabric via layer-by-layer assembly technique, RSC Adv. 6 (2016) 27669–27676.

[35] J.K. Oh, X.X. Lu, Y.J. Min, L. Cisneros-Zevallos, M. Akbulut, Bacterially antiadhesive, optically transparent surfaces inspired from rice leaves, ACS Appl. Mater. Interfaces 7 (2015) 19274–19281.

[36] P.M. Sivakumar, V. Prabhawathi, R. Neelakandan, M. Doble, Chalcone coating on cotton cloth - an approach to reduce attachment of live microbes, Biomater. Sci. 2 (2014) 990–995.

[37] S.G. Chen, L.J. Yuan, Q.Q. Li, J.N. Li, X.L. Zhu, Y.G. Jiang, et al., Durable antibacterial and nonfouling cotton textiles with enhanced comfort via zwitterionic sulfopropylbetaine coating, Small 12 (2016) 3516–3521.

[38] L. He, C. Gao, S. Li, C.T.W. Chung, J.H. Xin, Non-leaching and durable antibacterial textiles finished with reactive zwitterionic sulfobetaine, J. Ind. Eng. Chem. 46 (2017) 373–378.

[39] Q.H. Qiu, J.J. Wu, Z.Z. Quan, H.N. Zhang, X.H. Qin, R.W. Wang, et al., Electrospun nanofibers of polyelectrolyte-surfactant complexes for antibacterial wound dressing application, Soft Matter 15 (2019) 10020–10028.

[40] Y.J. Xi, T. Song, S.Y. Tang, N.S. Wang, J.Z. Du, Preparation and antibacterial mechanism insight of polypeptide-based micelles with excellent antibacterial activities, Biomacromolecules 17 (2016) 3922–3930.

[41] P. Canizares, I. Gracia, L.A. Gomez, A. Garcia, C.M. de Argila, D. Boixeda, et al., Thermal degradation of allicin in garlic extracts and its implication on the inhibition of the in-vitro growth of Helicobacter pylori, Biotechnol. Prog. 20 (2004) 32–37.

[42] A.R. Sarasam, R.K. Krishnaswamy, S.V. Madihally, Blending chitosan with polycaprolactone: effects on physicochemical and antibacterial properties, Biomacromolecules 7 (2006) 1131–1138.

[43] K.M. Sukhyy, E. Belyanovskaya, M.P. Sukhyy, Modification technology of montmorillonite by polyionenes, J. Chem. Technol. 26 (2018) 1–8.

[44] T. Pongprayoon, N. Yanumet, E.A. O'Rear, W.E. Alvarez, D.E. Resasco, Surface characterization of cotton coated by a thin film of polystyrene with and without a cross-linking agent, J. Colloid Interface Sci. 281 (2005) 307–315.

[45] H. Murata, R.R. Koepsel, K. Matyjaszewski, A.J. Russell, Permanent, non-leaching antibacterial surfaces - 2: how high density cationic surfaces kill bacterial cells, Biomaterials 28 (2007) 4870–4879.

[46] S.K. Samal, M. Dash, S. Van Vlierberghe, D.L. Kaplan, E. Chiellini, C. van Blitterswijk, et al., Cationic polymers and their therapeutic potential, Chem. Soc. Rev. 41 (2012) 7147–7194.

[47] Z. Li, D. Lee, X. Sheng, R.E. Cohen, M.F. Rubner, Two-level antibacterial coating with both release-killing and contact-killing capabilities, Langmuir 22 (2006) 9820–9823.

[48] M.Z. Zhang, J. Zhao, J. Zheng, Molecular understanding of a potential functional link between antimicrobial and amyloid peptides, Soft Matter 10 (2014) 7425–7451.

[49] J. Wu, J.J. Ye, J.J. Zhu, Z.C. Xiao, C.C. He, H.X. Shi, et al., Heparin-based coacervate of FGF2 improves dermal regeneration by asserting a synergistic role with cell proliferation and endogenous facilitated VEGF for cutaneous wound healing, Biomacromolecules 17 (2016) 2168–2177.

[50] J. Wu, J.J. Zhu, C.C. He, Z.C. Xiao, J.J. Ye, Y. Li, et al., Comparative study of heparin-poloxamer hydrogel modified bFGF and aFGF for in vivo wound healing efficiency, ACS Appl. Mater. Interfaces 8 (2016) 18710–18721.